
**ISAS - INTERNATIONAL SCHOOL FOR ADVANCED STUDIES**


# Selected topics in polymer physics

Thesis submitted for the degree of

"Doctor Philosophiæ"


CANDIDATE

Stefano Lise

SUPERVISOR

Prof. Amos Maritan


October 1998


**SISSA - SCUOLA INTERNAZIONALE SUPERIORE DI STUDI AVANZATI**

TRIESTE
Via Beirut 2-4

**TRIESTE**

SISSA ISAS
SCUOLA INTERNAZIONALE SUPERIORE DI STUDI AVANZATI
INTERNATIONAL SCHOOL FOR ADVANCED STUDIES

# Selected topics in polymer physics

Thesis submitted for the degree of

"Doctor Philosophiæ"

CANDIDATE

Stefano Lise

SUPERVISOR

Prof. Amos Maritan

October 1998

# Table of Contents

# Introduction

Polymers are the basic constituents of a wide variety of materials (both natural and artificial) having diverse applications in industry and daily life. The study of these macromolecules has a long history and continues to be one of great current interest.
Polymer physics began to develop in the 1930's under the influence of chemical and biological applications. It was progressively realized that the properties of a polymer at large length scales are determined essentially by the long chain structure, rather than by the detailed chemical nature of the molecules. A polymer in solution displays universal behavior analogous to that occurring in ferromagnets at the Curie temperature, in binary systems at the consolute point, in fluids at the liquid-gas critical point, etc. Its properties can accordingly be described by a restricted number of critical exponents. A major achievement in the field was the discovery by P.G. de Gennes (Nobel laureate in 1991) of a relationship between polymer statistics and phase transition in spin systems. This connection enabled polymer science to benefit from the vast progress made by the theory of critical phenomena. As a result of all the efforts, the equilibrium behavior of a flexible polymer in dilute solution is believed to be by now well understood. In a good solvent (at high temperature) the polymer is an expanded random coil, while in a poor solvent (at low temperature) it is a compact ball. The temperature separating these two phases is called $\theta$ temperature and, precisely at this temperature, the polymer is described by critical exponents different from those in either the good or poor solvent regimes.

One of the simplest (and most effective) models of a polymer is a a self-avoiding walk on a lattice, with an energy depending on the shape of the walk. Because of the universality hypothesis, in most of the theoretical studies concerning the $\theta$ transition, the interactions between monomers have been included in the simplest way: a pair of nearest neighbor monomers on the lattice interacts through an attractive potential, provided they are not consecutive along the chain.
Recently, however, the possible existence of more complex behavior has been suggested both by theory and by experiments. Indeed the growing interest of physicists toward molecular biology has revealed that this simple form of interaction is inadequate in the case of

biopolymers such as, for instance, proteins and DNA molecules.
This thesis explores simple generalization of the self-avoiding walk problem with the aim of approaching a better description of such complicated systems. We will verify that peculiar interaction mechanisms can influence the nature of the transition and induce a collapse towards different compact (and even non compact) phases. These possibilities imply a richer scenario and a wider degree of non universality than those contemplated in the usual $\theta$ point physics.

In chapter 1 we study the collapse transition of a linear homopolymer model, which presents two competing interactions: an attractive potential between pair of monomers and an energy penalty which discourages a single monomer from having more than a certain number of contacts. The first interaction favors the collapse of the chain, the second enhances the ramification into thin branch-like structures.
The model is directly inspired by a lattice model recently introduced to describe protein behavior and, in particular, to take into account that different amino acids have different sizes (and, therefore, a different capability of admitting surrounding molecules).
We study the phase diagram and the critical behavior of the system through exact enumerations and Monte-Carlo simulations. In addition we present an analytical argument which determines qualitatively the phase boundaries. Our findings suggest the existence of a complex phase diagram, with a swollen, a compact and a branched phase.

In chapter 2 we consider Hamiltonian walks on a lattice, i.e. self-avoiding walks that visit all the sites. As globular protein in their native state form compact structures, Hamiltonian walks have recently become one of the model of choice for protein folding studies.
We formulate the polymer problem in terms of a particular $O(n)$ model, in the limit $n \to 0$. We then use a suitable high-temperature expansion to estimate the total number of Hamiltonian walks on a lattice. This approach enables us to derive a mean-field result and to generate corrections to it in power of $1/d$ in a systematic way ($d$ is the dimensionality of the space). We calculate the coefficients of the series up to third order, extending of one order previous results.
The spin representation can be extended to Hamiltonian walks with a bending energy which favors straight segments of the chain. This is the so called Flory model for polymer melting. In this case, our mean field results are in agreement with approaches based on a field-theoretic representation of the partition function.

In chapter 3 we present a novel Bethe approximation to study lattice models of linear polymers. The approach is variational in nature and based on the cluster variation method. We apply it to study the phase diagram of a semiflexible chain model which includes both an attractive potential and a bending rigidity. This study should be relevant to the case of

stiff polymer, as for example DNA.
Our findings support the existence of an open coil at high temperature, a collapse globule at intermediate temperature and low stiffness, and a stretched phase at low temperature and large stiffness. The transition from the coil to the globule is a second order $\theta$ collapse, whereas the transition toward the stretched phase is a first order transition. We find evidences for a multicritical point, where the two transition lines meet. As a consequence, for sufficiently stiff polymers the globular phase disappears and the system undergoes a direct first order transition from the random coil to the orientational ordered state.
These results contradict in several aspects mean-field theory and are in good agreement with previous Monte Carlo simulations of the model.
In the limit of Hamiltonian walks, moreover, our approximation recovers results of the Flory-Huggins theory for polymer melting.

# 1 Polymers and Proteins

In this chapter we discuss some aspects of the statistical mechanics of lattice models of polymers and proteins.

The study of polymers has a long history and it is by now exhaustively covered by a number of text (see, for instance, [1, 2, 3, 4, 5]). The interest arises from the recognition that long polymer chains, despite the variety in their chemical composition and physical properties, behave in a universal manner when placed in solution. They provide therefore a very good example of critical behavior and, similarly to ferromagnet systems, they are characterized by universal exponents.

Proteins are compact objects with remarkably complex structures [6]. The protein folding problem is at the moment one the most fascinating and challenging open problems [7]. The aim is to apply methods developed in statistical mechanics for understanding the folding process and, in particular, the way the amino acids sequence determines the three dimensional structure of the protein [8].

In an attempt to make this thesis as self-contained as possible, we have devoted the first two paragraphs of this chapter to an introduction of simple concepts and definitions of polymers physics and proteins. At the same time, these paragraphs enable us to fix the relevant notation. We have limited ourselves to topics which will be useful in the following. We remand to the references listed in the bibliography for a more detailed treatment.

In the last section we present an investigation of a linear homopolymer model [9], which can be directly related to a model recently introduced to mimic protein behavior [10]. We investigate the effect of steric frustration on the collapse transition of a polymer. Our findings suggest the existence of a complex phase diagram, with a swollen, a compact and a branched phase.

## 1.1 Static properties of flexible polymers in solution

In this paragraph we will present a concise review of the equilibrium behavior of a polymer in a dilute solution, i.e. in a solution in which the volume available to each polymer is much larger than the volume it actually occupies. This limit enables to treat a single polymer as isolated, disregarding interactions between different polymers. We will also restrict ourselves to flexible polymers, leaving a discussion of the effect of chain stiffness to next chapters. We will focus in particular on the critical (i.e. universal) properties of a linear polymer like, for instance, the dependence of its typical extension on the linear length of the chain.

Polymers are macromolecules composed of a large number of monomer units, which are joined together by chemical bonds. A single monomer consists of a group of atoms, like, for instance, $CH_2$ in polyethylene. This is a chain molecule, whose skeleton is formed by a sequence of carbon atoms, each of which is coupled to two hydrogen atoms.

The relative orientation of two successive C-C bonds is essentially fixed to the tetrahedral angle $\theta \simeq 109.47$. A certain amount of freedom is instead left to the azimuthal angle $\phi$. Indeed the energy of rotation $E(\phi)$ has three deep minima, at $\phi = 0$ and $\phi \simeq \pm\pi/3$. The first orientation is referred to as the trans configuration; the two equivalent orientations at $\phi \simeq \pm\pi/3$ are called gauche configurations. When the energy difference between minima $\Delta\epsilon$ is smaller than the thermal energy $\kappa_B T$ ($\kappa_B$ is the Boltzmann constant, $T$ the absolute temperature) the relative weight of trans/gauche configurations is of order unity. The small local fluctuations on orientation accumulate along the chain and above a certain persistence length $l_p$ the directions of bonds become essentially uncorrelated. As long as $l_p$ is much smaller than the total length $L$, the polymer appears therefore as continuous and flexible at large scales.

Besides polyethylene, another simple example of homopolymer is polystyrene. This has the same carbon chain as a skeleton, but now of each four hydrogen atoms one is replaced by a hydrogenated carbon ring, so that the repeat unit is $CH_2CHC_6H_5$. In general monomers need not to be all identical: proteins and DNA molecules are typical example of heteropolymers. Proteins are made out of 20 amino acids, DNA molecules of 4 nucleotides.

The functionality of a monomer refers to the maximum number of chemical bonds a monomer can have. If the functionality of each monomer is 2, a linear polymer is formed; on the other hand, if some of the monomers have a higher functionality, a branched polymer can occur.

The number of monomers $N$ in a polymer is called degree of polymerization. In a linear polymer it can be of the order of $10^5$ or more. This implies that the length scale of the

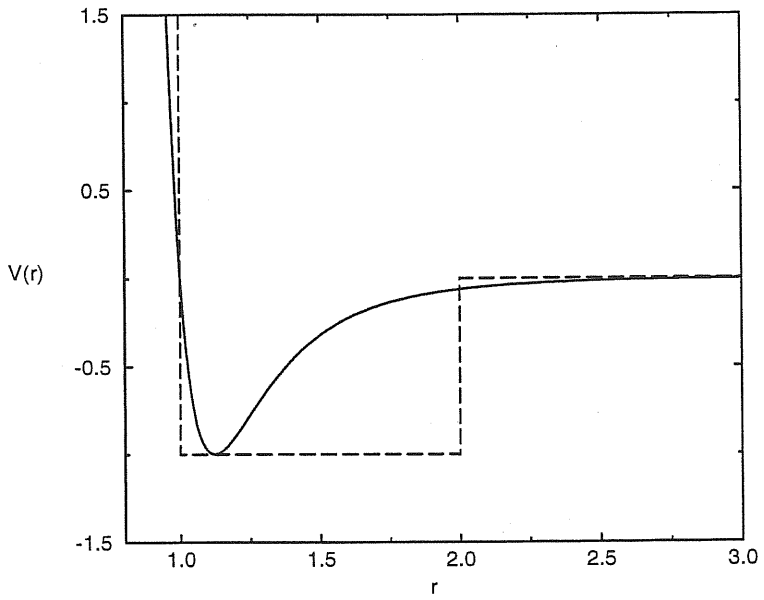


Figure 1.1: Schematic plot of the effective interaction $V$ between monomers as a function of the relative distance $r$ (continuous line). The dashed line represents the potential of an interacting self-avoiding walk on a lattice. Units are arbitrary.

entire polymer is macroscopic with respect to the length scale of the individual monomers (typically of the order of few Ångstrom). From a theoretical point of view it is therefore appropriate to consider the limit of infinite chain length ($N \to \infty$) and to employ statistical approaches even in the description of a single macromolecule.

Polymers are generally studied when immersed in solution. The energy of the system involves interactions between different monomers, between monomers and the molecules of the solvent and between the molecules of the solvent themselves. It is convenient most of the time to consider an effective interaction $V$ between monomers, which results by integrating the solvent degrees of freedom. Due to the enormous chemical variability in the local chemical structure of polymers, as well as the many possible choices of solvent, this interaction differs in detail from case to case, and moreover is seldom known explicitly. Its main feature, however, is that it is strongly repulsive at short distances, whereas it becomes weakly attractive at longer distances (see figure 1.1). The former characteristic gives rise to the so called excluded volume effect: the chance of finding a monomer in a region "close" to another monomer is rather low. The latter originates from Van der Waals forces between different monomers.

Polymers may exhibit several different types of morphology, depending on external condi-

tions such as temperature and chemistry of the solvent. At high temperatures the repulsive interactions are dominant. It is energetically more favorable for the monomers of the polymer to be surrounded by molecules of the solvent than by other monomers. This is the good solvent condition. The polymer assumes preferentially extended configurations with a large entropy. At low temperatures, instead, the effect of the attractive Vand der Waals potential comes into play. The quality of the solvent decreases and the monomer-monomer interactions are not efficiently screened. It corresponds to the bad solvent condition. The chain collapses into a compact object with little entropy. The transition point is usually referred to as the $\theta$ point. It is a continuous phase transition, where the energy of attraction balances the entropy difference between the two states.

One of the most important macroscopic observables for polymers is the radius of gyration $R_g$. It measures the average distance of the monomers from the center of mass. The radius of gyration of polymers can be determined experimentally, for example, from light scattering properties by an analysis of the structure factor. Of particular interest is the dependence of $R_g$ on the molecular weight or alternatively on the degree of polymerization. Such dependence gives informations on the macroscopic conformation of the polymer. It is expected to obey an asymptotic scaling law of the form

$$R_g \simeq aN^{\nu} \quad \text{for } N \to \infty \tag{1.1}$$

In (1.1) the amplitude $a$ depends on the microscopic details of the system such as the specific form of the intermolecular interactions. In contrast the exponent $\nu$ appears to a large extent universal. It is the same for all polymers and the details of chemical structure and interaction energy are irrelevant. It depends only on few, rather general parameters such as the temperature and the quality of the solvent. The different behaviors at large length scale of polymers in solution can accordingly be divided into a small number of universality classes. Typical values in three dimensions are $\nu \simeq 0.6$ for a polymer in a good solvent, $\nu = 1/3$ in a bad solvent and $\nu = 1/2$ at the $\theta$ point. It is important to underline that the exponent $\nu$ for the radius of gyration is believed to be the same for any measure of the extension of the polymer (e.g., the average end-to-end distance), since, due to universality, polymers are expected to have only one macroscopic length scale.

An extremely simple model which captures the essential physics of a linear, flexible polymer in solution is the self-avoiding walk (SAW) on a lattice. An $N$–step self-avoiding walk is an ordered sequence of $(N+1)$ vertices of the lattice with coordinates $\mathbf{r}_i$ $(i = 0, \ldots, N)$, such that $\mathbf{r}_0$ is the origin, pairs of vertices whose index differs by unity are unit distance apart, and every vertex is distinct (see [11] for a discussion of SAW). The SAW model aims to a coarse-grained description of polymers, that is on length scales much longer than the persistence length. Indeed the lattice spacing represents a distance of the order of $l_p$ and

details on the monomer scale are ignored. With a slight abuse of notation, in the following we will refer to the vertices of the walk as 'monomers', although, strictly speaking, each of them already corresponds to a collection of 'real' monomers.

Real polymers live in spatial dimension $d = 3$ (ordinary polymer solutions) or in some cases in $d = 2$ (polymer monolayers confined to an interface). Nevertheless, it is convenient to define and study the SAW model on a general hypercubic lattice. This approach permits to understand the important role played by dimensionality, in analogy with ordinary critical phenomena (e.g. the ferromagnetic transition in the Ising model). A SAW is an infinitely flexible random walk which never intersects itself. The self avoiding constraint takes into account the excluded volume repulsion. The longer range Van der Waals interactions are also generally considered. They are easily mimicked by assigning a negative energy $-\epsilon_v$ (in some unit) to each contact of the walk. A contact is defined as a pair of monomers which are nearest neighbor on the lattice but which are not joined by a step of the SAW. This interaction potential is certainly microscopically not realistic (see figure 1.1) but it yields the correct scaling behavior, as long as we are interested in universal quantities. Its choice is dictated by mere theoretical and computational convenience.

Let $\beta = \frac{1}{\kappa_B T}$ be the inverse temperature. The partition function of the system reads

$$Z_N = \sum_{\{S\}} e^{\beta \epsilon_v N_{con}(\mathcal{S})} \tag{1.2}$$

where $\{S\}$ denotes the ensemble of all $N$–step SAW and $N_{con}(\mathcal{S})$ is the number of non-bonded contacts in walk $\mathcal{S}$. For large $N$ it is believed to scale as

$$Z_N \simeq \mu^N N^{\gamma-1} \tag{1.3}$$

This relation defines the entropic exponent $\gamma$, which, similarly to the exponent $\nu$, is expected to be universal and to take on three distinct values[1]. On the other hand, the connectivity constant $\mu$ is system dependent.

The $\theta$ transition has in recent years attracted much theoretical interest, mostly in connection with universality issues. Depending on the value of the parameter $\omega = \beta\epsilon_v$, the interacting SAW presents three different universal regimes, in agreement with experimental results.

*Coil Phase.* For low values of $\omega$, the chain has an expanded, swollen structure. The critical behavior is governed by the fix point of the pure SAW (i.e. $\omega = 0$), whose connectivity constant on different lattices is reported in table 1.1. A simplified mean-field argument

[1] In $d = 2$ the universality of the exponent $\gamma$ in the compact phase is still debated. It seems to be very sensitive both to the lattice under investigations and to the boundary conditions involved. See chapters 7 and 8 in [5] for a discussion.

| lattice | $\mu$ |
|---|---|
| square | $2.638159 \pm .000002$ [12] |
| hexagonal | $1.847759 \pm .000006$ [13] |
| triangular | $4.15080 \pm .00003$ [14] |
| cubic | $4.68393 \pm .00006$ [14] |

Table 1.1: The connectivity constant $\mu$ for SAW on different lattices.

given by Flory predicts for the exponent $\nu$

$$\begin{aligned} \nu &= \tfrac{3}{d+2} \quad \text{for } d < 4 \\ \nu &= \tfrac{1}{2} \quad \text{for } d \geq 4 \end{aligned} \tag{1.4}$$

The system is described by the exponents of the ideal random walk above $d = 4$, which therefore is the upper critical dimension of the problem. The Flory values for $\nu$ are known to be correct for $d = 1$ and $d \geq 5$ and they are believed to be correct for $d = 2$ and $d = 4$ as well. The estimate for $d = 3$ is instead believed to be *only* an excellent approximation: numerical and field theory calculations indicate $\nu \approx 0.59$. It is important to underline that the remarkable success of Flory's argument is somewhat fortuitous. The self-consistent calculation in fact benefits from the simultaneous cancellation of two estimates which are incorrect (see page 46 of [2] for a brief discussion).

*Globular Phase* For high values of $\omega$, the chain collapses into a compact configuration. The spatial density of monomers is finite and, accordingly, the radius of gyration scales as $R_g \sim N^{1/d}$, which implies $\nu = 1/d$.

*$\theta$ point.* At the $\theta$ value of $\omega$ ($\omega_\theta$), the system undergoes a phase transition. In $d = 2$ the collapse transition occurs at $\omega_\theta \simeq 0.66$[15], in $d = 3$ at $\omega_\theta \simeq 0.28$[16]. It is a trictritical point [17] and hence the upper critical dimension of the phenomenon is $d_c = 3$. An extension of the Flory argument to include the effect of the attractive interactions give

$$\begin{aligned} \nu &= \tfrac{2}{d+1} \quad \text{for } d < 3 \\ \nu &= \tfrac{1}{2} \quad \text{for } d \geq 3 \end{aligned} \tag{1.5}$$

In $d = 2$ it predicts $\nu = 2/3$ whereas the presumably exact value is $\nu = 4/7$[18].
In table 1.2 we give a summary of the values that the exponents $\nu$ and $\gamma$ have in distinct universality classes.

We conclude this paragraph with a brief survey of known results about branched polymers (BP). Branched polymers are often modeled by lattice trees or lattice animals. A lattice tree is a connected set of bonds which has no closed loops; a lattice animal is a

| dimension | $d=2$ | $d=3$ |
|---|---|---|
| | good solvent | |
| $\nu$ | 3/4[19] | $0.5877 \pm .0006$ [20] |
| $\gamma$ | 43/32[19] | $1.157 \pm .003$[21] |
| | $\theta$ point | |
| $\nu$ | 4/7[18] | 1/2 |
| $\gamma$ | 8/7[18] | 1 |

Table 1.2: The critical exponent $\nu$ for the interacting SAW. Presumably exact values are reported as simple fraction.

connected cluster of bonds which may contain closed loops[2]. A quantity of interest is the radius of gyration $R_g$, which is believed to scale for large $N$ as

$$R_g \sim N^{\nu} \tag{1.6}$$

for some critical exponent $\nu$ which is expected from universality to be the same for both trees and animals. A second critical exponent is defined through the number of $N$-bonds trees and/or animals, denoted respectively by $t_N$ and $g_N$. The asymptotic behavior of these quantities is believed to be of the form

$$t_N \sim \mu_t^N N^{-\theta} \quad g_N \sim \mu_g^N N^{-\theta} \tag{1.7}$$

again with the same critical exponent $\theta$. In $d=2$ the connectivity constant is $\mu_t \simeq 5.140$ for lattice trees and $\mu_g \simeq 5.212$ for lattice animals; in $d=3$, $\mu_t \simeq 10.496$ and $\mu_g \simeq 10.633$ (for references see [5]).
The upper critical dimension for these models is 8, above which the mean field exponents ($\nu = 1/4$ and $\theta = 5/2$) are correct. We list results (exact and numerical) for $d=2$ and $d=3$ in table 1.3.

| d | 2 | 3 | 4 | 8 |
|---|---|---|---|---|
| $\theta$ | 1 | 3/2 | 11/6 | 5/2 |
| $\nu$ | $0.64075 \pm .00015$ | 1/2 | 5/12 | 1/4 |

Table 1.3: Critical exponents for BPs. The numerical value is taken from [22], whereas the exact exponents have been derived by Parisi and Sourlas [23]

[2]An equivalent digression can be given in term of site animals. For simplicity we consider only bond animals

## 1.2 The protein folding problem

In this section we will review the equilibrium thermodynamics of proteins, placing particular emphasis on the properties of simple lattice models. Such models provide a coarse-grained description of proteins and, contrary to higher-resolution models, they are amenable to an exact classification of the phase space. A different approach, which involves the "thermodynamic limit" (i.e. number of monomers going to infinity) will be considered in next chapters.

A protein is a linear heteropolymer, which consists of a particular sequence of monomers. These are chosen among the 20 naturally occurring amino acids. The amino acids are of different types, often grouped according to their interactions with water (their natural solvent). They are therefore classified either as hydrophobic or as hydrophilic. Some of the amino acids may also be weakly charged. The typical size of a protein ranges from approximately 100 amino acids for small proteins to 500 for long immuno-globulins.

Proteins may exist in different phases, depending on external conditions such as temperature, nature of the solvent and pH of the solution. The most important state of a globular protein is known as the native or folded state. In this state the protein has its full biological activity. Proteins are in their native states in aqueous solvents near neutral pH at $20 - 40$ C; indeed this is the typical cellular environment. Each protein has a unique native state, which is determined completely by the sequence of amino acids. It has an extremely compact and well defined three dimensional structure: it is (probably) the configuration which minimizes the energy of the system. The conformational entropy of the native state is basically zero. Under some non physiological conditions, such as high temperature, acidic or basic pH, or in some non aqueous solvents, the unique folded structure of a protein reversibly unfolds or denatures and, as a consequence, the protein looses its biological activity. Depending on chemical conditions, it seems that it can exist in at least two distinct denaturated phases: the coil state and the molten globule. The coil state is a phase with a large conformational entropy. The protein assumes an expanded conformation, which resembles the swollen phase of a homopolymer in a good solvent. The molten globule is a compact, globular phase with finite conformational entropy. Contrary to the native state, it does not have a well defined structure and it bears strong resemblance to the collapsed phase of a homopolymer in a bad solvent. Some proteins may exist in the molten globule at low pH (acidic conditions).

Different proteins have different sequences of amino acids, which are held together by covalent bonds. The amino acid sequence along the main backbone chain is known as the primary structure of a protein. The secondary structure refers to the regular structures that form on a local scale. These structures are stabilized by hydrogen bonds and can

be of two different types: $\alpha$ helices and $\beta$ sheets. Roughly speaking, $\alpha$ helices have one dimensional order, whereas $\beta$ sheets have two dimensional order. There are on average 3.6 amino acids per helix turn and the typical size of a helix is 5 turns. A typical strand in a $\beta$ sheet has a length of 8 amino acids and there are approximately 3 strands in a $\beta$ sheet. The tertiary structure is the full three dimensional structure of the protein, obtained by arranging conveniently in space secondary structures.

The protein folding problem consists in understanding the relationships between amino acids sequences and native structures. It can be formulated from two distinct, complementary perspectives: the direct and the inverse folding problem. The direct folding aims at predicting the compact three dimensional structure of the native state from knowledge of the monomer sequence. On the other hand the inverse folding tries to determine the amino acid sequence which folds into a desired native structure. Solving the inverse folding problem would be of great importance to biotechnology, as the biological function of a protein is mainly controlled by its shape. It would therefore enable the design of new drugs with desired functionality.

Simple lattice models have often been employed to explore the sequence-structure relationship. In this perspective proteins are represented at a rudimentary level, as SAW on lattices. Each bead of the walk corresponds to an amino acid and, in general, only interactions between nearest-neighbor (non bonded) monomers are included. Despite some clear oversimplifications they are able to capture some of the essential, general principles involved in protein folding, possibly providing a more global (less atomistic) view of the problem.

Perhaps the most popular of such models is the HP model [24]. This model has its physical basis in the consideration that hydrophobic interactions are the dominant driving forces for the collapse of proteins. In fact non polar amino acids have a strong tendency to associate in water. They therefore create an hydrophobic core in the interior of the molecule, leaving hydrophilic monomers to reside preferentially on the surface of the globule (although exceptions are common). In the HP model proteins are modeled by SAWs on a square or cubic lattice. Each protein is represented by a specific sequence of hydrophobic (H) and polar (P) monomers. There is an attractive interaction between pair of H monomers which are adjacent in space but not covalently linked. For P-P pairs and P-H pairs, instead, the interaction energy is zero. In recent years this model has been the object of numerous investigations, using both exact enumerations and Monte Carlo simulations. In general, the results found are largely in agreement with the behavior of real proteins. In particular:
(i) The lowest energy states are typically compact with H monomers on the interior and shielded from the solvent.
(ii) Only a small fraction of sequences admit a unique ground state (apart from obvious ro-

tations), in agreement with the non-random nature of the amino acid sequence in proteins.
(iii) A significant number of different structures (i.e. configurations of the SAW) are the unique ground state of one or more sequences. These structures are called encodable and reflect the diversity of shape (and hence of biological function) observed in proteins.
(iv) Some of the native structures can be encoded by a large number of different sequences. These particular structures are therefore highly designable, being the non degenerate ground state of several sequences. This property is consistent with the ability of a protein to retain its structure even when small changes to the sequence are brought.

More recently a different lattice model has been introduced, the LS model [10]. This model takes into account another structural principle, related to the severe steric constraints which are present in a protein. Indeed different amino acids have different sizes and therefore a different capability of admitting surrounding molecules. In this sense it complements the perspective from the HP model. In its simplest version the LS model consists of two type of monomers, denoted by L (large) and S (small). Steric constraints are included by postulating that, in order to accommodate the large size of an L amino acid, at least one of the sites next to it must be kept vacant. The amino acids of the S type, instead, have no such constraint. Monomers of the chain interact through a short range attractive potential, regardless of their L or S nature. In terms of interactions therefore the model is completely similar to that of an homopolymer, with the energy proportional to the number of non bonded contacts. The model has been exhaustively studied on the two dimensional square lattice, revealing many of the desirable attributes for modeling proteins. Indeed for a chain of length 16 there are 7555 sequences (out of $2^{16} = 65536$) with a unique ground state. Remarkably 7202 of such sequences have a maximally compact native state with no voids in the interior. There are 117 distinct encodable structures, 33 of which are maximally compact. Moreover the maximum number of sequences which fold on the same ground state (the maximum designability score) is 519. For comparison, we report in table 1.4 a summary of the results for the HP and the LS models, on two dimensions for length $N = 12$ and $N = 16$.

In general simple lattice models suffer of obvious disadvantages:
(i) They are crude low-resolution representations of proteins, which do not include any atomic detail. They often use only two monomer types, rather than 20.
(ii) They consider a minimal set of interactions, describing the energy of the system not accurately.
(ii) They have a few discrete values for bond angles, dictated by the structure of the underlying lattice.
(iii) They consider length of the chains up to about 30 monomers. These are much shorter

| Model | N | ES | CES | MDS |
|---|---|---|---|---|
| LS | 12 | 15 | 15 | 24 |
| HP | 12 | 25 | 5 | 14 |
| LS | 16 | 117 | 33 | 519 |
| HP | 16 | 456 | 20 | 26 |

Table 1.4: Comparison between the HP and the LS models on the square lattice. The chain length is N, the number of encodable structures is ES, the number of compact encodable structures is CES and the maximum designability score is MDS. The results for the LS model are taken form [10]; the results for the HP model have been presented in [25].

than real proteins.
(iv) They are sometimes restricted to a two dimensional space. As for the previous point, this is due to computational limitations.

On the other hand, these models are undoubtedly of great interest. Despite such shortcomings, in fact, they offer some advantages. We list a few:
(i) They may allow complete enumerations of the full conformational and sequence spaces. Alternatively, they allow to use efficient methods to sample accurately the phase space. This is not always possible using atomic-level simulations, which require molecular dynamics techniques.
(ii) They involve a small number of parameters. The direct consequences of a model are therefore easier to understand.
(iii) They capture some physical properties more faithfully in 2D rather than in 3D. This is the case, for instance, for the surface-volume ratio, which is a principal factor in the physics of folding. In order to reproduce the correct ratio for a molecule of the size of myoglobin, a chain of 154 monomers is needed in 3D, but only of about $16 - 20$ monomers in 2D.
(iv) They involve the least microscopic detail, allowing to deduce general principles of protein structure and stability.

## 1.3 A lattice model for homopolymers with steric frustration

In this section we present an investigation of a two dimensional homopolymer model, which represent a simple generalization of the interacting SAW discussed in the first paragraph of this chapter. The model is directly inspired by the LS model for protein folding in the way it takes into account steric effects. We will find that it exhibits a rich phase diagram with

a swollen, a compact and a branched polymer phase.

For the sake of simplicity we consider the model on a square lattice, but generalization to different lattices and/or higher dimensions is also possible. Let $i = 0 \ldots N$ be the coordinate of the vertices along the walk and let $\mathbf{r}_i$ denotes the location of the $i$-th monomer. A pair of non consecutive vertices in the chain ($|i-j| \neq 1$) interacts through an attractive nearest-neighbor ($|\mathbf{r}_i - \mathbf{r}_j| = 1$) potential $\omega$. This would be the standard lattice model studied for the collapse transition of linear polymers. In addition, we have included an effect of steric frustration by assigning an energy penalty $\epsilon$ to each monomer $i$ with four nearest-neighbor sites occupied (including possibly monomers $i+1$ and $i-1$). The partition function of the model can be written as

$$Z_N = \sum_{m,l} C_N(m,l) \mathrm{e}^{\omega \mathrm{m} - \epsilon \mathrm{l}} \tag{1.8}$$

where $C_N(m,l)$ denotes the number of distinct $N$-step SAWs with $m$ contacts and $l$ 'frustrated' monomers. For $\epsilon = 0$ the model reduces to a standard attractive SAW: it undergoes a $\theta$ collapse at a critical $\omega_c \approx 0.66$ [15]. In the limit $\epsilon \to \infty$, instead, each monomer is forced to have at most three nearest-neighbor sites occupied. The polymer therefore optimizes its energy by arranging itself in two parallel straight segments at a distance of one (in lattice units). This consideration suggests that for small enough temperatures (and $\epsilon = \infty$) the polymer could prefer a branched structure (on a coarse-grained level).

The model defined by the partition function (1.8) is very similar to a model introduced and studied by Dekayser et al. [26] in a different context. The difference between the two models is indeed restricted to the form of the interaction favoring ramification: in [26] a fugacity $y$ was given to every step of the walk having two parallel steps at unit distance. We expect this difference to be irrelevant, so that the two models should present the same scaling behavior.

We have first studied the phase diagram of the system as a function of $\epsilon$ and $\omega$ with the method of exact enumeration. This is a numerical approach which involves a complete determination of all distinct SAWs up to a certain finite length. It provides therefore exact finite size values for the quantities of interest, such as the radius of gyration $R_N$ defined through

$$R_N^2 = \frac{1}{N} \sum_{i=0}^{N} \langle (\mathbf{r}_i - \bar{\mathbf{r}})^2 \rangle \tag{1.9}$$

where $\bar{\mathbf{r}} = \frac{1}{N} \sum_{i=0}^{N} \mathbf{r}_i$ is the center of mass and the angular brackets denotes an average over configurations. The results are then extended to the limit $N \to \infty$ by inferring an asymptotic behavior and by using extrapolation techniques, as for instance the ratio method and the method of Pade' approximants [27]. By means of a backtracking algorithm we have performed exact enumerations of SAW up to $N = 28$ step, extending the $N = 26$ steps

analysis reported in [26]. We have determined the series of $C_N(m,l)$ and $R_N(m,l)$, where $R_N(m,l)$ is the average radius of gyration of an $N$–step SAW having $m$ contacts and $l$ frustrated monomers. From these quantities the (thermal) expectation value for the radius of gyration of the polymer can be easily computed as

$$R_N^2(\omega,\epsilon) = \frac{\sum_{m,l} C_N(m,l) R_N^2(m,l) e^{\omega m - \epsilon l}}{\sum_{m,l} C_N(m,l) e^{\omega m - \epsilon l}} \tag{1.10}$$

To avoid parity effects we have grouped separately even and odd lengths and then formed effective exponents $\nu_{\mathrm{N}}$ through the relation

$$2\nu_{\mathrm{N}}(\omega,\epsilon) = \frac{\ln \frac{R_N^2}{R_{N-2}^2}}{\ln \frac{N}{N-2}} \tag{1.11}$$

Let us consider first the simpler case $\epsilon = 0$. In a infinite system $\nu_{\mathrm{N}}$ is expected to be a step function as a function of $\omega$, with a discontinuity at the $\theta$ point, $\omega_\theta$. In a finite system, however, the shape is rounded and it approaches a step function only as $N$ increases. We denote with $\Delta\omega = \omega - \omega_\theta$. In the neighborhood of the critical region $\Delta\omega \to 0$ and $N \to \infty$, the following scaling relation for a tricritical point is expected to hold

$$R_N^2 \simeq N^{2\nu_\theta} F(\Delta\omega N^{\phi}) \tag{1.12}$$

where the scaling function $F(x)$ satisfies

$$\begin{aligned} F(x) &\to x^{2\frac{\nu_{SAW}-\nu_\theta}{\phi}} \quad \text{for } x \to \infty \\ F(x) &\to x^{2\frac{\nu_{gl}-\nu_\theta}{\phi}} \quad \text{for } x \to -\infty \end{aligned} \tag{1.13}$$

with $\nu_{gl} = 1/d$. The exponent $\phi$ is the so called crossover exponent. Scaling theory, therefore, asserts that at $\omega_\theta$ (where $\Delta\omega = 0$) the value of $\nu_{\mathrm{N}}$ is independent of $N$ and it is equal to $\nu_\theta$. Although in principle relation (1.12) holds only for $N \to \infty$, it has proven to be valuable in identifying the transition point even for finite $N$.

We have applied a crossover form like (1.12) to investigate the general case $\epsilon \neq 0$. In figure 1.2 we have plotted $\nu_{\mathrm{N}}$ for different $N$ values as a function of $\omega$ for (a) $\epsilon = 0.2$ and (b) $\epsilon = \infty$. As they do not intersect in a single point, in order to locate the transition point we have considered the dispersion of the $\nu_{\mathrm{N}}$ curves. For a set of $M$ curves, each of which labeled by an index $i = 1, \ldots, M$, this quantity is defined as

$$\sigma = \frac{1}{M} \sum_i (\nu_{\mathrm{N_i}} - \overline{\nu}_{\mathrm{N}})^2 \tag{1.14}$$

with

$$\overline{\nu}_{\mathrm{N}} = \frac{1}{M} \sum_i \nu_{\mathrm{N_i}} \tag{1.15}$$

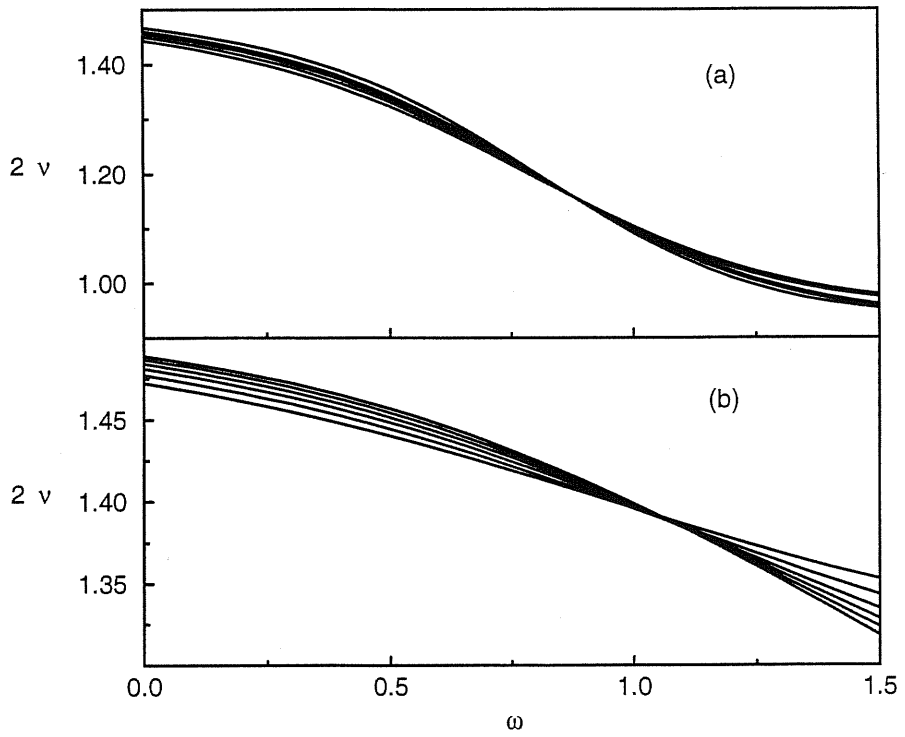


Figure 1.2: Exact enumeration results for the effective exponent $\nu_N$ as a function of $\omega$ for (a) $\epsilon = 0.2$ and (b) $\epsilon = \infty$. The lengths are $N = 18, 20, 22, 24, 26, 28$. Similar plots result from considering odd lengths.

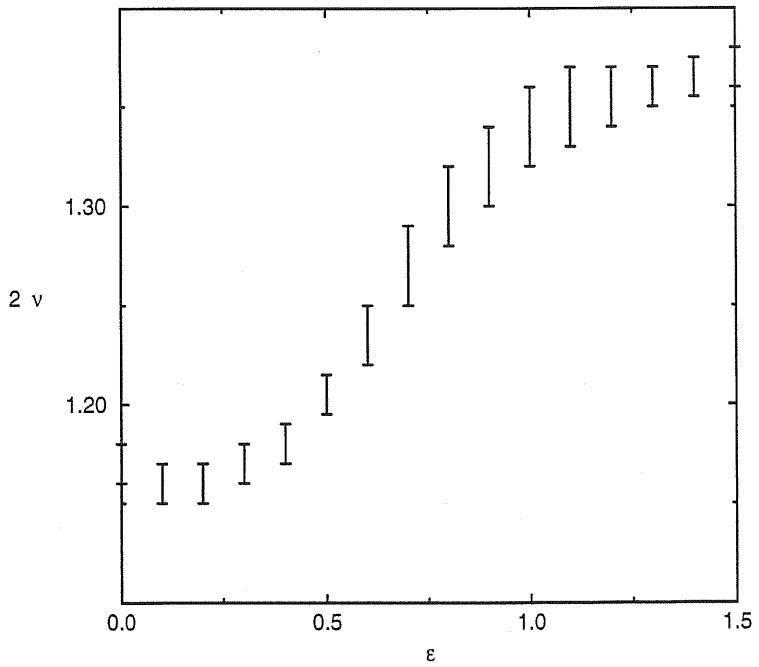


Figure 1.3: Behavior of the correlation length exponent $\nu$ along the compact–swollen and branched–swollen transition line, as obtained from series.

In both cases of fig. 1.2(a) and (b) there is a point where the dispersion $\sigma$ has a pronounced minimum, signaling the presence of a transition from a high to a low temperature phase [28]. We have taken the coordinates of this point to be the critical $\omega$ and the value of the exponent $\nu$ at the collapse transition. The dispersion (1.14) has been used to estimate the error. In fig. 1.3 we have reported the behavior of $\nu$ along the transition line as a function of $\epsilon$. For small values of $\epsilon$ the critical exponent is $\nu = 0.58 \pm 0.01$, whereas by further increasing $\epsilon$ it seems to move to a different value. This is an indication that a transition from a swollen to a branched phase takes place. Universality class considerations suggest that the curve of fig. 1.3 ideally should be a step function and the rounded shape is just a crossover effect. All the points in the transition line from the swollen to the compact phase presumably belong to the universality class of the $\theta$–collapse of a linear polymer, so that the correlation length exponent is $\nu_{s-c} \approx 0.57$. Similarly one can predict that the transition from swollen to branched polymer is dominated by a different unique fixed point, which determines the critical exponents $\nu_{s-b}$ $(0.64 \leq \nu_{s-b} \leq 0.75)$.

The complete phase diagram obtained from series analysis is shown in figure 1.4 as isolated points. This is in good agreement with the phase diagram reported in [26]. The relatively large error bars on the points determining the compact–branched transition reflect the

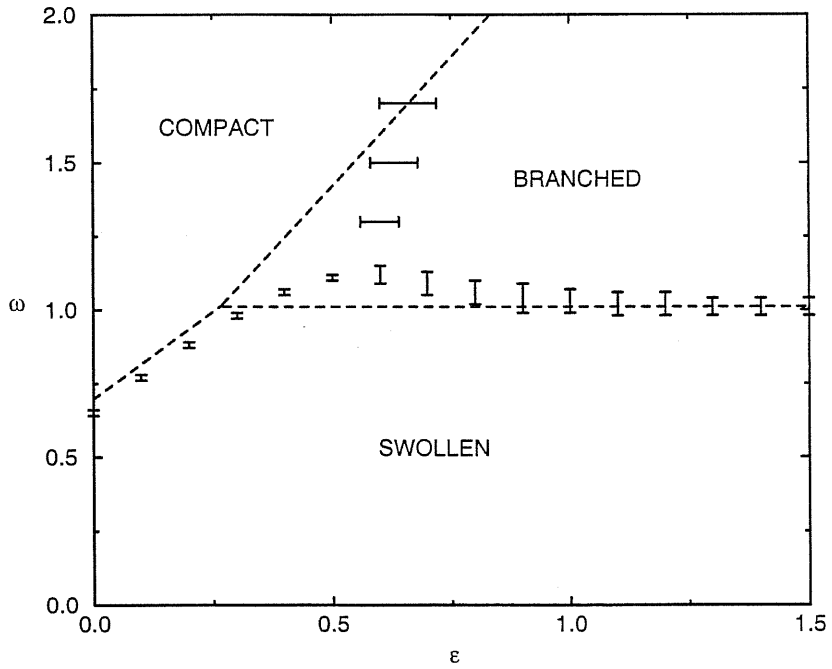


Figure 1.4: Phase diagram of the system as a function of $\omega$ and $\epsilon$. The isolated points are obtained from series analysis. The dashed line is the conjecture from heuristic calculations.

intrinsic difficulty of using series to describe such a transition [29]. Indeed most of the $\nu_N$ curves do not intersect, although a region where their distance has a pronounced minimum is visible. For this reason we have complemented the analysis by looking at a thermal quantity such as the specific heat per monomer, defined through the relation

$$C = \frac{1}{N}\left(\langle E^2\rangle - \langle E\rangle^2\right) \tag{1.16}$$

where $E$ denotes the reduced energy of the system. The corresponding curves show a peak which grows and sharpens with increasing $N$, possibly indicating the presence of a phase transition (see figure 1.5).

The phase behavior of the system could also be conjectured from the following heuristic argument, based on energy–entropy balance. We assume the polymer can be in three different phases (swollen, compact and branched) and we estimate the corresponding free energies by the competition between energy and entropy.

(i) *Swollen phase.* The average number of contacts $< m >$ in a noninteracting SAW is $< m > \sim aN$, with $a \approx 0.16$ [30], whereas the total number of SAWs scales as $N_{\mathrm{SAW}} \sim \mu_{\mathrm{SAW}}^N$, where $\mu_{\mathrm{SAW}} \approx 2.64$ [12] is the connectivity constant of the SAWs. For sufficiently high

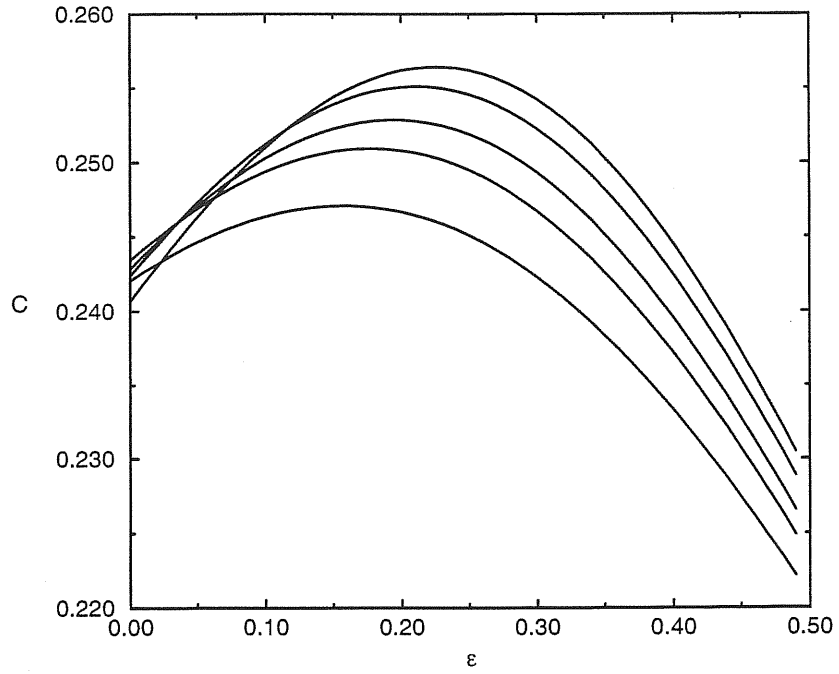


Figure 1.5: Specific heat per monomer as a function of $\epsilon$ for $\omega = 1.5$. The lengths are $N = 20, 22, 24, 26, 28$.

temperatures, the free energy of the swollen phase is therefore reasonably approximated by

$$\beta F_{\rm s} \simeq -aN\omega - N \ln \mu_{\rm SAW} \tag{1.17}$$

where $\beta = 1/\kappa_B T$. In principle one should also include in (1.17) a contribution proportional to $\epsilon$. We have determined from series the average number of vertices with four nearest neighbor sites occupied $< l >$. It scales like $< l > \sim bN$, with $b \simeq 0.03$ and it is therefore negligible.

(ii) *Compact phase.* The compact phase of a polymer can be suitably modeled by a Hamiltonian walk, which is a space filling SAW visiting all sites of a lattice of linear size $N^{\frac{1}{2}}$ (in $d = 2$). In this limit

$$\beta F_{\rm c} \simeq -N(\omega - \epsilon) - N \ln \mu_{\rm HW} \tag{1.18}$$

since each monomer has four nearest-neighbor sites occupied and the number of non bonded contacts is exactly $N$, apart from non-extensive surface contributions. The connectivity constant could be taken to be $\mu_{HW} = \frac{4}{e}$, which is a mean-field approximation in very good agreement with the exact value [31][3].

[3]We discuss the properties of Hamiltonian walks in next chapter

(iii) *Branched phase.* In the limit $\epsilon \to \infty$, the free energy of the branched phase is roughly

$$\beta F_{\rm b} \simeq -\frac{N}{\alpha}\omega - \frac{N}{\alpha}\ln \mu_{\rm BP} \tag{1.19}$$

with $\mu_{\rm BP} \sim 5.21$ [32]. The factor $\alpha$ in equation (1.19) arises from the peculiar structure of the branched polymer, which makes the effective length of the chain shorter and, at the same time, forces a certain number of contacts between monomers. Although $\alpha$ can be easily inferred to be between 2 and 3, a precise determination of its value eludes us. For this reason we have set $\alpha \simeq 2.35$, in order to fit the branched–swollen transition asymptotically, as determined from series analysis. The broken lines in the phase diagram of figure 1.4 result from comparing expressions (1.17)–(1.19) as a function of $\omega$ and $\epsilon$. The stable phase is determined by the lowest value of the free energy.

To estimate the value of the critical exponent $\nu_{\rm s-b}$ accurately we have considered the case $\epsilon = \infty$ separately. In this limiting case, all sites of the walk are prevented from having more than three occupied neighboring sites (including bonding neighbors). The analysis from the series expansion lead us to quote $\nu = 0.70 \pm 0.01$ (see figure 1.2(b)). We have complemented the analysis by carrying out Monte Carlo simulations. This is a numerical method which allows to treat chains longer than the exact enumeration approach. It samples randomly the space of SAW configurations, with a probability proportional to the correct Boltzmann weight. It therefore provides statistical estimates and confidence intervals for the quantity of interest.

There are a large number of distinct Monte Carlo procedure (for a review see [33]). In our study we have implemented a pivot algorithm [34, 35]. The pivot algorithm picks a "pivot site" at random on the current walk, breaks the walk into two pieces at that site, and then applies a randomly chosen symmetry operation of the lattice to one piece, using the pivot site as the origin. If the resulting walk is self-avoiding, it is accepted according to the Metropolis acceptance/rejection test[4]; otherwise it is rejected. Probably the pivot algorithm is presently the most accurate algorithm for simulating SAW. It has been used to simulate SAW of length up to 80000 steps in $d = 2$ and $d = 3$ [20]. In $d = 2$ these calculations confirm the predicted exponent $\nu = 3/4$; in $d = 3$ lead to the estimate $\nu = 0.5877 \pm 0.0006$.

Unfortunately the efficiency of the algorithm dramatically decreases at low temperatures. The acceptance rate is very low and the chain spends long periods sampling relatively small regions of the configuration space and only rarely move to other regions. In order to circumvent this problem we have implemented a multiple Markov chain method [16]. With this method we run parallel simulations at $m$ (of the order of 10) different temperatures

[4] Let $E(X)$ and $E(X')$ be the reduced energy of the old and new configurations respectively. The configuration $X'$ is accepted with a probability equal to $\min(1, \exp(E(X) - E(X'))$.

($\beta_1 < \ldots < \beta_m$). After every $N_{sw}$ Monte Carlo steps we select, with uniform probability, a pair of configurations at adjacent temperatures $\beta_i$ and $\beta_{i+1}$, and we try to interchange them. The trial move is accepted with a weight that ensures that the limiting distributions at the $m$ different temperatures are indeed the Boltzmann distributions. The clear advantage of this method is that it enables large changes in the configuration space.

The Monte Carlo technique allowed an accurate calculation of the square gyration radii for walks up to 45 sites with an estimated error of at most 1% for $0 < \beta < 1.2$. Moreover it turned out to be in excellent agreement with the series results obtained for $N$ up to 28. The values of $\nu$ were obtained by first performing a smoothing procedure [36], in order to reduce the stochastic noise. We have considered the coefficient $b_N$ defined as a sum over an increasing number of $R_N^2$

$$b_N = \sum_{i=10}^{N} R_N^2 \tag{1.20}$$

They should scale asymptotically as $b_N \sim N^{2\nu+1}$. By identifying the crossing of the curves pertaining to length $N$ and $N+8$ we identified the values of $\nu_{N+4}$. Plotting $\nu_N$ against $1/N$ shows a marked linear behavior, the correlation coefficient being $r \approx -0.85$. By linear regression we extrapolated the asymptotic value $\nu_{N\to\infty}$ obtaining $\nu_{s-b} = 0.695 \pm 0.006$, in good accordance with the series analysis.

The model in [26] was analyzed by means of a similar exact enumerations technique. There is, nonetheless, a discrepancy on the value of the critical exponent $\nu_{s-b}$. The authors in [26] have quoted $\nu_{s-b} \simeq 0.65$, which does not appear to be compatible with our estimate. We will come back to this point in the Conclusions of the thesis, in connection also with other models which display the same SAW-BP transition.

# 2 Hamiltonian walks on a lattice

In this chapter we discuss the properties of a polymer which occupies a finite fraction $f$ of sites (dense polymers). In particular we will be interested in the case $f = 1$, i.e. in space filling self-avoiding walks. These are often referred to as Hamiltonian walks and their properties have recently attracted much interest [37, 38, 39]. We will also investigate the effects of a residual stiffness on the chain. In this form the model is known as the Flory model for polymer melting [40, 41].

In the first paragraph we fix notations and definitions. We also derive a formal relation between the Flory model and a particular spin model. By performing a Gaussian transformation we verify that the spin representation is in fact equivalent to a field theoretical representation devised in [31, 42].
In paragraph 2 we estimate the total number of Hamiltonian walks on a lattice through a suitable high-temperature expansion of the spin model. We calculate a mean-field result and $1/d$ corrections to it up to third order.
We conclude (paragraph 3) with a mean field investigation of the Flory model.

## 2.1 The Flory Model. Spin and field theoretical representation

We consider a $d$-dimensional hypercubic lattice with $N = L^d$ sites and periodic boundary conditions. An Hamiltonian walk (HW) is defined as a self-avoiding walk, which visits all sites of the lattice once and only once. For simplicity, in the following we will restrict ourselves to closed paths, whose length is therefore precisely $N$ (in lattice units).

Hamiltonian walks have been largely investigated as a model for the configurational statistics of compact polymer structures (see [5, 43]). In the simplest version, each HW is equally weighted and they are believed to describe collapsed polymer globules. Namely, the total number of HWs corresponds to the entropy of the polymer in a collapsed but disordered phase. More complex systems can also be modeled by including a weight that depends on

the shape of the cycle. The Flory model, for instance, considers a bending rigidity which favors straight segments of the chain. This is achieved by associating an energy $\epsilon_h > 0$ to each pair of consecutive monomers which are not collinear. This model is believed to capture some of the essential features of the melting of semiflexible polymer chains (see also [44]). The system is expected to undergo a phase transition between a high–temperature disordered state and a low–temperature ordered state. The latter is characterized by anisotropic orientational order and henceforth will be denoted as a solid phase, whereas the former is the analogous of a liquid phase. In passing, it is worthwhile to mention that the Flory model finds a natural interpretation also in the context of the protein folding problem [45, 46, 47]. This point will be pursued further in the following chapter.

The partition function of the Flory model at inverse temperature $\beta = \frac{1}{\kappa_B T}$ reads

$$Z = \sum_{\{H\}} e^{-\beta \epsilon_h N_c(\mathcal{H})} \tag{2.1}$$

where $\{H\}$ denotes the ensemble of all Hamiltonian walks and $N_c(\mathcal{H})$ is the number of corners in walk $\mathcal{H}$. In the particular case $\beta\epsilon_h = 0$ (i.e. zero stiffness or infinite temperature) the partition function (2.1) counts the total number of HWs ($\mathcal{N}_H$). In the limit $N \to \infty$, this number scales exponentially with the number of monomers as $\mathcal{N}_H \simeq \mu_H^N$ (see equation (1.3)), where $\mu_H$ is the connectivity constant. In the ground state (at $T = 0$) the polymer is instead completely ordered and all bonds are parallel to one axis of the lattice. The model therefore presents a competition between rigidity and entropy effects.

We derive in this section a formal relation between HWs and spin models. This is done in close analogy to the De Gennes theorem for SAW [48]. The advantage of the formulation through spin variables is that it allows the application of standard techniques of statistical mechanics, such as mean-field theory and high-temperature expansion.

In order to establish the connection between HWs and spin models, we consider $n$-components vectors and we associate $d$ of such vectors to each site $\mathbf{r}$ of the lattice

$$\mathbf{S}_\alpha(\mathbf{r}) = \left(S_\alpha^1(\mathbf{r}), \ldots, S_\alpha^n(\mathbf{r})\right) \tag{2.2}$$

We denote with $\alpha = 1, \ldots, d$ the possible directions and with $\hat{\alpha}$ the corresponding unit vectors.
We then introduce a trace operation over the variables $S_\alpha^i(\mathbf{r})$, which is defined formally as

$$\mathrm{Tr} = \prod_{\mathbf{r}} \mathrm{tr}_{\mathbf{r}} = \prod_{\mathbf{r}} \int \prod_{i,\alpha} dS_\alpha^i(\mathbf{r}) \rho(\mathbf{S}(\mathbf{r})) \tag{2.3}$$

where $\rho(\mathbf{S}(\mathbf{r}))$ is a suitable measure which satisfies

$$\mathrm{tr}\ 1 = \mathrm{tr}\ S_\alpha^i = \mathrm{tr}\ S_{\alpha_1}^{i_1} \ldots S_{\alpha_k}^{i_k} = 0 \quad \text{if } k \neq 2 \tag{2.4}$$

and

$$\text{tr } S_\alpha^i S_\beta^j = \delta_{i,j} \begin{cases} 1 & \text{if } \alpha = \beta \\ \exp(-\beta\epsilon_h) & \text{if } \alpha \neq \beta \end{cases} \tag{2.5}$$

Notice that tr $1 = 0$ which is a quite unusual property. Given these definitions, the partition function (2.1) can be written as

$$Z = \lim_{n\to 0} \frac{1}{n} \text{Tr } \exp\left[\frac{1}{2} \sum_{\mathbf{r},\mathbf{r}'} \sum_{\alpha} \Delta^{\alpha}_{\mathbf{r},\mathbf{r}'} \mathrm{S}_\alpha(\mathbf{r}) \mathrm{S}_\alpha(\mathbf{r}')\right] \tag{2.6}$$

where

$$\Delta^{\alpha}_{\mathbf{r},\mathbf{r}'} = \begin{cases} 1 & \text{if } \mathbf{r} - \mathbf{r}' = \pm\hat{\alpha} \\ 0 & \text{otherwise} \end{cases} \tag{2.7}$$

and, as usual

$$\mathrm{S}_\alpha(\mathbf{r})\mathrm{S}_\alpha(\mathbf{r}') = \sum_{i=1}^{n} S_\alpha^i(\mathbf{r}) S_\alpha^i(\mathbf{r}') \tag{2.8}$$

Equation (2.6) is formally equivalent to the partition function of a spin system. This connection will be largely exploited in next paragraphs.

To prove the identity (2.6) we expand the partition function in a power series as follows

$$Z = \lim_{n\to 0} \frac{1}{n} \text{Tr} \prod_{\mathbf{r},\alpha} \left[1 + \mathrm{S}_\alpha(\mathbf{r})\mathrm{S}_\alpha(\mathbf{r}+\hat{\alpha}) + \frac{1}{2}\left(\mathrm{S}_\alpha(\mathbf{r})\mathrm{S}_\alpha(\mathbf{r}+\hat{\alpha})\right)^2\right] \tag{2.9}$$

Because of the properties of the trace (2.4), higher order terms do not contribute to the expansion (2.9). It is convenient to represent the terms in (2.9) graphically, indicating which links contribute to a particular term. In this view, each factor in square brackets can be visualized either by an empty bond (weight 1), by an occupied bond (weight $\mathrm{S}_\alpha(\mathbf{r})\mathrm{S}_\alpha(\mathbf{r}+\alpha)$ or by a double occupied bond (weight $(\mathrm{S}_\alpha(\mathbf{r})\mathrm{S}_\alpha(\mathbf{r}+\alpha))^2$). The product (2.9) becomes therefore a sum over all possible bond configurations, over which the trace operation has to be taken.

Consider, for example, the case of all empty bonds (all bond variables equal to 1). As a direct consequence of the definition (2.4), the trace operation gives zero. The same result holds for a configuration with an isolated site, that is is a configuration with no spin variables associate to that site. Indeed, the trace operation factories as a product over single site traces. For the same property, configurations with a site having 1, 3 or more nearest-neighbor connections have no weight. The only graphs which survive are those which have exactly two links attached to each site. These are therefore closed self-avoiding walks (also called self-avoiding polygons) which cover the whole lattice[1]. Because of (2.5),

[1]Due to the quadratic term in (2.9), polygons of length 2 are also included

each polygons has a weight $e^{-\beta\epsilon_h}$ associate to each corner. Each connected component (loop), moreover, yields a factor $n$. The factor $1/n$ combined with the limit $n \to 0$ enables to extract the contribution of paths making just one loop. Each term in the diagrammatic expansion corresponds therefore to a Hamiltonian walk with the correct weight and this concludes the proof.

A field theoretical expression of the partition function was considered in [42]. It reads

$$Z = \lim_{n\to 0} \frac{1}{n} \int \prod_{\alpha} d\varphi_\alpha(\mathbf{r}) e^{-A_G} \prod_{\mathbf{r}} \frac{1}{2} \left( \sum_{\alpha} \varphi_\alpha^2(\mathbf{r}) + e^{-\beta\epsilon_h} \sum_{\alpha\neq\beta} \varphi_\alpha(\mathbf{r})\varphi_\beta(\mathbf{r}) \right) \tag{2.10}$$

with

$$A_G = \frac{1}{2} \sum_{\alpha=1}^{d} \sum_{\mathbf{r},\mathbf{r}'} \varphi_\alpha(\mathbf{r}) (\Delta^\alpha_{\mathbf{r},\mathbf{r}'})^{-1} \varphi_\alpha(\mathbf{r}') \tag{2.11}$$

where $\varphi_\alpha(\mathbf{r})$ is an $n$-component real field, defined in each direction $\alpha = 1, \ldots, d$ and attached to all points $\mathbf{r}$ of the lattice. The two formulations, (2.6) and (2.10), are equivalent and related by an Hubbard-Stratonovich transformation. Indeed, by performing a Gaussian integral on the partition function (2.6) we find

$$Z = \lim_{n\to 0} \frac{1}{n} \mathrm{Tr} \, \frac{\int \prod_{\mathbf{r}} \prod_{\alpha} d\varphi_\alpha(\mathbf{r}) e^{-A_G + \sum_\alpha \sum_{\mathbf{r}} \varphi_\alpha(\mathbf{r}) \mathbf{S}_\alpha(\mathbf{r})}}{\int \prod_{\mathbf{r}} \prod_{\alpha} d\varphi_\alpha(\mathbf{r}) e^{-A_G}} \tag{2.12}$$

The difficulty associated with the non positive definiteness of the matrix $\Delta^\alpha_{\mathbf{r},\mathbf{r}'}$ could be removed by adding an harmless constant term to it. Indeed it would introduce a term proportional to $\sum_{\mathbf{r},\alpha} \mathbf{S}^2_\alpha(\mathbf{r})$ to the exponent in (2.6). However, in the $n \to 0$ limit, $Z$ is indipendent on this term. The trace over the $\mathbf{S}$ variables can now be computed as

$$\mathrm{tr} \, e^{\sum_\alpha \varphi_\alpha(\mathbf{r}) \mathbf{S}_\alpha(\mathbf{r})} = \frac{1}{2} \left( \sum_{\alpha} \varphi_\alpha^2(\mathbf{r}) + e^{-\beta\epsilon_h} \sum_{\alpha\neq\beta} \varphi_\alpha(\mathbf{r})\varphi_\beta(\mathbf{r}) \right) \tag{2.13}$$

Moreover, in the limit $n \to 0$ the denominator is equal to 1, so that the expression (2.10) is recovered.

## 2.2 Enumeration of Hamiltonian walks. Mean field theory and $1/d$ corrections

It is known that high-temperature expansions performed at a fixed order parameter (like the magnetization for a ferromagnet) provide a simple and reliable way to derive mean-field theory and corrections to it [49, 50]. For instance, the ordinary mean-field theory for the Ising model is recovered with just the first two terms in the expansion of the magnetization-dependent free energy (i.e. the Gibbs potential). Similarly, the Thouless, Anderson and

Palmer (TAP) free energy for spin glasses is obtained by including terms up to the second order [2] . Higher order terms in the expansion have been used to successfully generate $1/d$ corrections to mean-field, both for the Ising model and for the Sherrington-Kirkpatrick model [50].

In this section we will perform a similar high-temperature expansion for HWs. We will consider only the particular case of zero stiffness ($\epsilon_h = 0$), where we need to consider just one $n$-dimensional vector attached to each site, instead of $d$. The partition function (2.6) in fact simplifies to

$$Z = \lim_{n\to 0} \frac{1}{n} \mathrm{Tr}\ \exp\left[\sum_{<\mathbf{r},\mathbf{r}'>} \mathbf{S}(\mathbf{r})\mathbf{S}(\mathbf{r}')\right] \tag{2.14}$$

where the sum in the exponential is over nearest neighbor pairs. This approach will enables us to derive a mean-field approximation for the total number of HWs and to generate corrections to it in power of $1/d$ in a systematic way.

We begin by constructing the following magnetization dependent free energy

$$-A\left[\beta, \{\mathbf{m}\}\right] = \ln \mathrm{Tr}\ \exp\left[\beta \sum_{<\mathbf{r},\mathbf{r}'>} \mathbf{S}(\mathbf{r})\mathbf{S}(\mathbf{r}') + \sum_{\mathbf{r}} \lambda(\mathbf{r})\left(\mathbf{S}(\mathbf{r}) - \mathbf{m}(\mathbf{r})\right)\right] \tag{2.15}$$

The trace operation is defined analogously to the previous section, i.e. tr $S^i S^j = \delta_{ij}$ is the only non zero term. The Lagrange multipliers $\lambda(\mathbf{r})$ act as external magnetic fields and they depend on the inverse temperature $\beta$ and on the local magnetization $\mathbf{m}(\mathbf{r})$. They have been introduced to fix the magnetization at each site $\mathbf{r}$ to its thermal average $\mathbf{m}(\mathbf{r}) =< \mathbf{S}(\mathbf{r}) >$, where, for any operator $O$, the $\langle\ \rangle$ brackets denote the canonical expectation value

$$\langle O \rangle = \frac{\mathrm{Tr}\ O \exp\left[\beta \sum_{<\mathbf{r},\mathbf{r}'>} \mathbf{S}(\mathbf{r})\mathbf{S}(\mathbf{r}') + \sum_{\mathbf{r}} \lambda(\mathbf{r})\left(\mathbf{S}(\mathbf{r}) - \mathbf{m}(\mathbf{r})\right)\right]}{\exp\left[\beta \sum_{<\mathbf{r},\mathbf{r}'>} \mathbf{S}(\mathbf{r})\mathbf{S}(\mathbf{r}') + \sum_{\mathbf{r}} \lambda(\mathbf{r})\left(\mathbf{S}(\mathbf{r}) - \mathbf{m}(\mathbf{r})\right)\right]} \tag{2.16}$$

At the end of the calculation, we will set $\beta = 1$ and we will also require

$$\frac{\partial A\left(\beta, \{\mathbf{m}\}\right)}{\partial \mathbf{m}(\mathbf{r})} = \lambda(\mathbf{r}) = 0 \tag{2.17}$$

These conditions ensure our results will indeed apply to the partition function (2.14) and, as a consequence, to HWs.

Before carrying on with the computation, we derive a useful relation between $\mathbf{m}(\mathbf{r})$ and $\lambda(\mathbf{r})$ at $\beta = 0$. We denote with $\langle\ \rangle_0$ an average taken at $\beta = 0$. In this case the expectation values

[2]The TAP free energy is presumably exact for an infinite-ranged spin glass model. This model (also known as the Sherrington-Kirkpatrick model) is expected to give a mean-field description of spin glasses.

are those of a non-interacting system. Since $\mathbf{m}(\mathbf{r})$ are held constant and do not depend on $\beta$, they are in particular equal to $< \mathbf{S}(\mathbf{r}) >$ when $\beta = 0$, implying

$$\mathbf{m}(\mathbf{r}) =< \mathbf{S}(\mathbf{r}) >_0 = 2\frac{\lambda(\mathbf{r})}{\lambda(\mathbf{r})^2} \tag{2.18}$$

or, equivalently

$$\lambda(\mathbf{r}) = 2\frac{\mathbf{m}(\mathbf{r})}{\mathbf{m}(\mathbf{r})^2} \tag{2.19}$$

We now expand $A(\beta, \mathbf{m})$ around $\beta = 0$ using a Taylor expansion

$$A(\beta) = A(0) + \left.\frac{\partial A}{\partial \beta}\right|_{\beta=0} \beta + \left.\frac{\partial^2 A}{\partial \beta^2}\right|_{\beta=0} \frac{\beta^2}{2} + \dots \tag{2.20}$$

where we have temporarily suppressed the dependence of $A$ on $\{\mathbf{m}\}$. The zeroth order term of the expansion is

$$A(0) = \sum_{\mathbf{r}} \left(\lambda(\mathbf{r})\mathbf{m}(\mathbf{r}) + \ln\frac{2}{\lambda(\mathbf{r})^2}\right) = \sum_{\mathbf{r}} \left(2 + \ln\frac{\mathbf{m}(\mathbf{r})^2}{2}\right) \tag{2.21}$$

The first derivative in equation (2.20) gives

$$\left.\frac{\partial A}{\partial \beta}\right|_{\beta=0} = -\langle \sum_{<\mathbf{r},\mathbf{r}'>} \mathbf{S}(\mathbf{r})\mathbf{S}(\mathbf{r}')\rangle_0 = -\sum_{<\mathbf{r},\mathbf{r}'>} \mathbf{m}(\mathbf{r})\mathbf{m}(\mathbf{r}') \tag{2.22}$$

The second derivatives in $\beta$ is

$$\left.\frac{\partial^2 F}{\partial \beta^2}\right|_{\beta=0} = -dN\frac{\mathbf{m}^4}{4}n \tag{2.23}$$

and hence it vanishes in the limit $n \to 0$. In deducing (2.23) we have exploited the homogeneity of the system, so that $\mathbf{m} \equiv \mathbf{m}(\mathbf{r})$ does not depend on $\mathbf{r}$. Higher order corrections are most easily evaluated with the aid of diagrams consisting of one bond, two bonds, etc. Each bond represents a $\beta$ term, whereas the vertices represent functions of the $\mathbf{m}(\mathbf{r})$. We discuss details of the calculation in the appendix 1.

The high temperature expansion (2.20) can be converted into an expansion in powers of $1/d$. The diagrams of the series can in fact be sorted according to the order at which they first contribute to a $1/d$ expansion for $A$. In general $d^{-r}$ corrections require up to $2r$-bond diagrams. By including all terms which contribute to order $1/d^3$, we obtain for the magnetization dependent free energy

$$\frac{A}{N} = 2 + \ln\frac{\mathbf{m}^2}{2} - d\mathbf{m}^2 + \frac{d\mathbf{m}^6}{12} - \frac{d^2\mathbf{m}^8}{8} + \frac{d\mathbf{m}^8}{8} - \frac{d^2\mathbf{m}^{10}}{8} + \frac{d^3\mathbf{m}^{12}}{12} + O(\frac{1}{d^4}) \tag{2.24}$$

The magnetization is determined from the thermodynamic relation (2.17). By requiring the first derivatives of $A$ with respect to $\mathbf{m}^2$ vanishes at any order, we obtain

$$\mathbf{m}^2 = \frac{1}{d}(1 - \frac{1}{4}\frac{1}{d^2} + \frac{3}{8}\frac{1}{d^3} + \ldots) \tag{2.25}$$

Substituting these results into (2.24) we derive a $1/d$ expansion for the free energy density

$$\frac{A}{N} = \ln\frac{\mathrm{e}}{2d} - \frac{1}{24}\frac{1}{d^2} + \frac{1}{12}\frac{1}{d^3} + \ldots \tag{2.26}$$

which in turn yields a $1/d$ expansion for the connectivity constant of HWs[3]

$$\mu_H = \frac{2d}{e}\left[1 + \frac{1}{24}\frac{1}{d^2} - \frac{1}{12}\frac{1}{d^3} + O(\frac{1}{d^4})\right] \tag{2.27}$$

The mean-field result corresponds to the leading order in (2.27) and, as for ordinary spin systems, it is recovered by including just the first two terms in the expansion (2.20). Expression (2.27) is in agreement with the findings of Orland et al. (who calculate it up to $d^{-1}$ corrections) [31] and Nemirovsy et al. (up to $d^{-2}$ order) [51]. It extends of one order previous results, which were obtained starting from two distinct field-theoretic representations. Moreover it compares very well with numerical estimates, probably because first order corrections vanishes. For the square lattice, for instance, Batchelor et al. [52] and Kondev et al. [38] using transfer matrix techniques have quoted $\mu_H \simeq 1.4728$. The mean-field value is $\mu_H^{(MF)} = 1.4715$ and by including the second order correction becomes $\mu_H^{(2)} = 1.4868$; the third order correction exactly cancel second order term, so that $\mu_H^{(3)} = \mu_H^{(MF)} = 1.4715$. Figure 2.1 displays the connectivity constant $\mu_H$ as a function of the coordination number $q = 2d$ for increasing order in $q^{-1}$. Exact and best numerical estimates are also reported.

## 2.3 Mean field theory for the Flory model

Mean field theories can be formulated in several different ways. In the previous section, for example, we have derived it from a suitable high-temperature expansion. An alternative, variational derivation is based on the Gibbs-Bogoliubov inequality. Let $H$ be the microscopic Hamiltonian of a system and $F$ the corresponding free energy. It can then be proved that

$$F \leq F_0 + \langle H - H_0\rangle_0 \equiv \tilde{F} \tag{2.28}$$

where $H_0$ is a trial Hamiltonian, $F_0$ the corresponding free energy and $\langle\ldots\rangle_0$ denotes an average taken in the canonical ensemble defined by $H_0$. It is customary to choose trial

[3]There is a subtle question related to the $1/n$ factor in 2.14. In a mean field theory based on a field theoretic representation [31], this factor is correctly cured by the degeneracy of the saddle point solutions (of the order $O(n)$). We have not been able to find a simple argument for it in our case.

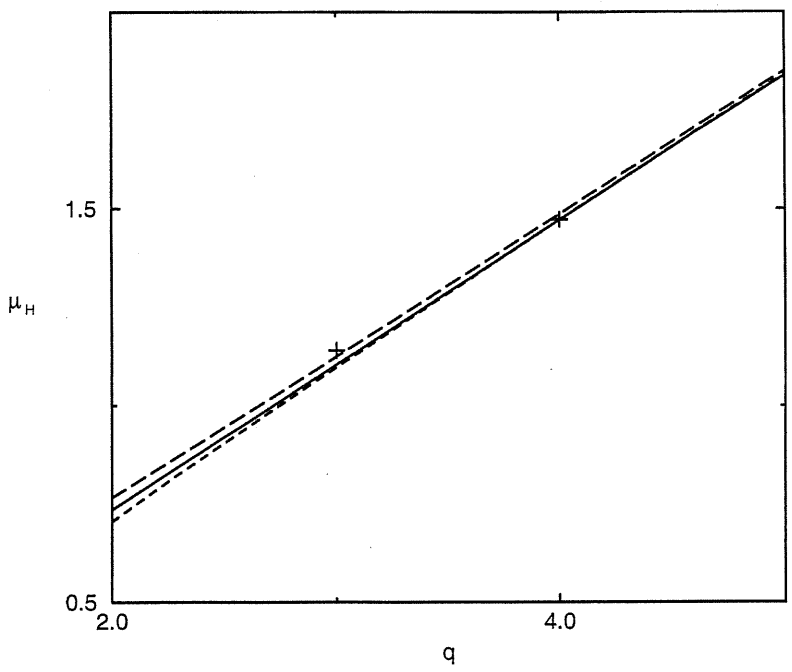


Figure 2.1: Connectivity constant $\mu_H$ for Hamiltonian walks as a function of the coordination number $q = 2d$. The curves shown are the mean field (solid line), the second order (long-dashed line) and the third order (dashed line) results. The crosses stand for results on the hexagonal ($q = 3$) and square ($q = 4$) lattices. The first is exact [53], whereas the second is numerical [38, 52]

Hamiltonians which depend on a set of parameters $\{B\}$ and which enable explicit calculation of the right-hand side of the inequality. The mean-field free energy is then defined by minimizing $\tilde{F}$ with respect to the variational parameters $\{B\}$.

$$F_{MF} = \min_{\{B\}} \tilde{F} \tag{2.29}$$

In this section we present a mean-field approach to the Flory model (2.6), based on the inequality (2.28). Our results are in agreement with mean-field theories based on the field-theoretic representation (2.10). These approaches evaluate the free energy of the system by saddle-point methods on the functional integral [42, 47].

The usual choice for a mean-field approximation is a non-interacting trial Hamiltonian

$$H_0 = \sum_{\mathbf{r}} \sum_{\alpha=1}^{d} \mathbf{B}_\alpha(\mathbf{r}) \mathbf{S}_\alpha(\mathbf{r}) \tag{2.30}$$

where $\mathbf{B}_\alpha(\mathbf{r})$ is an $n$-component vector. In principle, the most general single site Hamiltonian would also include a term of the form[4] $\left(\sum_{ij} M^{ij}_{\alpha\beta} S^i_\alpha S^j_\beta\right)$. However, we have verified that, after minimizing $\tilde{F}$, $M^{ij}_{\alpha\beta} = 0$, so that in the following we do not include it for notational clarity.

The partition function corresponding to (2.30) can be easily calculated

$$\begin{aligned} F_0 &= -\ln Z_0 = -\ln \mathrm{Tr}\ \mathrm{e}^{H_0} = \\ &= -N \ln \left[ \frac{1}{2} \sum_{\alpha=1}^{d} \mathbf{B}_\alpha^2 + \frac{\mathrm{e}^{-\beta\epsilon_h}}{2} \sum_{\alpha\neq\beta} \mathbf{B}_\alpha \mathbf{B}_\beta \right] \end{aligned} \tag{2.31}$$

To obtain equation (2.31) we have exploit the fact that the system we are considering is translationally invariant. The other terms contributing to the mean field free energy are

$$\langle H_0 \rangle_0 = \frac{\mathrm{Tr}\ \sum_{\mathbf{r},\alpha} \mathbf{B}_\alpha(\mathbf{r}) \mathbf{S}_\alpha(\mathbf{r}) \mathrm{e}^{H_0}}{\mathrm{Tr}\ \mathrm{e}^{H_0}} = 2N \tag{2.32}$$

and

$$\langle H \rangle_0 = \frac{\frac{1}{2} \sum_{\mathbf{r},\mathbf{r}',\alpha} \Delta^{\alpha}_{\mathbf{r},\mathbf{r}'} \mathbf{S}_\alpha(\mathbf{r}) \mathbf{S}_\beta(\mathbf{r}') \mathrm{e}^{H_0}}{\mathrm{Tr}\ \mathrm{e}^{H_0}} = \tag{2.33}$$

$$= Nd \frac{\sum_\alpha \left[ \mathbf{B}_\alpha + \mathrm{e}^{-\beta\epsilon_h} \sum_{\beta\neq\alpha} \mathbf{B}_\beta \right]^2}{\left[ \frac{1}{2} \sum_\alpha \mathbf{B}_\alpha^2 + \frac{\mathrm{e}^{-\beta\epsilon_h}}{2} \sum_{\alpha\neq\beta} \mathbf{B}_\alpha \mathbf{B}_\beta \right]^2} \tag{2.34}$$

Summing up equations (2.31), (2.32) and (2.33), we obtain an expression for $\tilde{F}$ as a function of $\{\mathbf{B}\}$. Because of the bending energy, we expect the polymer at low enough temperatures

[4] Higher order terms do not contribute to the trace operation

might order along one direction. It appears therefore natural to distinguish between one special direction and the remaining $d-1$ directions, so that the isotropic symmetry of the system can be broken. We label the vector associated to the preferred direction as $\mathbf{B}_1$ and denote all the remaining vectors equivalently as $\mathbf{B}$. It results in a lengthy expression

$$\begin{aligned}\frac{\beta\tilde{F}}{N} = & -\ln\left[\frac{\mathbf{B}_1{}^2}{2}+\frac{d-1}{2}\mathbf{B}^2+e^{-\beta\epsilon_h}(d-1)\mathbf{B}_1\mathbf{B}+\frac{\mathrm{e}^{-\beta\epsilon_h}}{2}(d-1)(d-2)\mathbf{B}^2\right] \\ & -\frac{\left[\mathbf{B}_1+(d-1)\mathrm{e}^{-\beta\epsilon_h}\mathbf{B}\right]^2+(d-1)\left[\mathbf{B}+\mathrm{e}^{-\beta\epsilon_h}\mathbf{B}_1+(d-2)\mathrm{e}^{-\beta\epsilon_h}\mathbf{B}\right]^2}{\left[\frac{\mathbf{B}_1{}^2}{2}+\frac{d-1}{2}\mathbf{B}^2+\mathrm{e}^{-\beta\epsilon_h}(d-1)\mathbf{B}_1\mathbf{B}+\frac{\mathrm{e}^{-\beta\epsilon_h}}{2}(d-1)(d-2)\mathbf{B}^2\right]^2} \\ & +2 \end{aligned} \tag{2.35}$$

In order to obtain the mean field free energy, we need to find the stationary points of equation (2.35) with respect to $\mathbf{B}$ and $\mathbf{B}_1$. Because of the $n \to 0$ limit and the peculiar definition of the trace operation, they turn out to be saddle points rather than local minima.

There is a liquid-like and a solid-like phase, corresponding respectively to the isotropic ($\mathbf{B}_1 = \mathbf{B}$) and the anisotropic ($\mathbf{B}_1 \neq \mathbf{B}$) solutions of the equation for stationary points. Their free energies are respectively

$$\frac{\beta F_L}{N} = -\ln\left[\frac{2(1+(d-1)\mathrm{e}^{-\beta\epsilon_h})}{\mathrm{e}}\right] = -\ln\frac{q_L(\beta\epsilon_h)}{\mathrm{e}} \tag{2.36}$$

and

$$\frac{\beta F_S}{N} = -\ln\left[\frac{2(1-\mathrm{e}^{-\beta\epsilon_h})}{\mathrm{e}}\right] = -\ln\frac{q_S(\beta\epsilon_h)}{\mathrm{e}} \tag{2.37}$$

Note that $q_L(\beta)$ and $q_S(\beta)$ play the role of an effective coordination number. In the case $\beta\epsilon_h = 0$, $q_L$ correctly recovers the mean field result $q = 2d$ (obtained from (2.27) in the limit $d \to \infty$). At $\beta\epsilon_h = \infty$, instead, $q_L = q_S = 2$ and the path is fully stretched. In figure 2.2 are reported $F_L$ and $F_S$ as a function of $(\beta\epsilon_h)^{-1}$ for $d = 3$. The disordered phase has always a lower free energy. On the other hand, there is a temperature $T_m$ at which $q_L(\beta\epsilon_h) = \mathrm{e}$, below which the free energy becomes positive. As the free energy of the Flory model is necessarily negative[5], one can infer there is a first order transition between a high temperature phase ($T > T_m$) and a low temperature phase ($T < T_m$), which, in this view, is just the ground state of the system. The melting temperature is given by

$$T_m = \frac{\epsilon_h}{\ln\left[\frac{2(d-1)}{\mathrm{e}-2}\right]} \tag{2.38}$$

[5]The ground state free energy per site vanishes. Since the free energy is a decreasing function of temperature ($\partial F/\partial T = -S$), it remains negative at all temperature

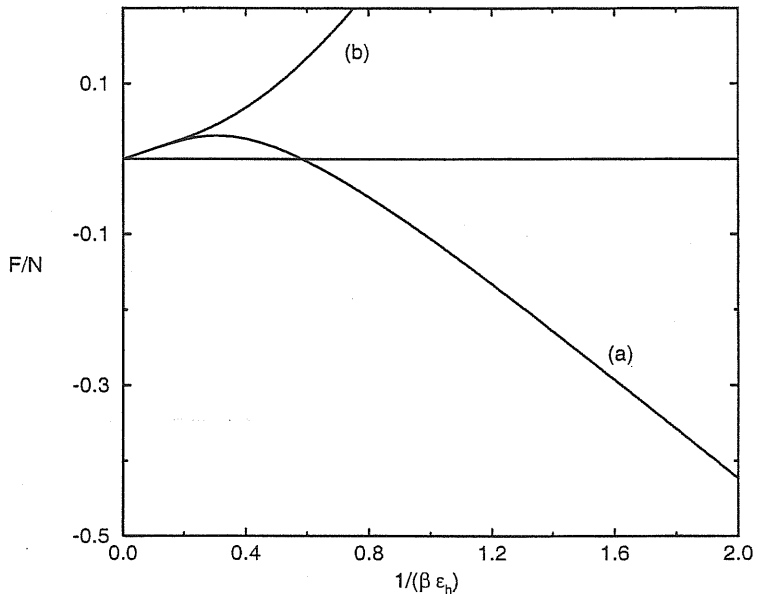


Figure 2.2: Mean field free energy of the Flory model in the (a) liquid phase and (b) solid phase for $d = 3$.

In $d = 2$ it occurs at $T_m \simeq 0.98\epsilon_h$, in $d = 3$ at $T_m \simeq 0.58\epsilon_h$.

In [42] a different mean field approach (named anisotropic mean field (AMF)) has also been considered. In this approach one direction in space is treated exactly and a mean field approximation is made on the remaining $(d-1)$ directions. In this way the one dimensional character of the low temperature phase is maintained and a first order transition between a fully stretched phase and a disordered phase is indeed found. In $d = 3$, $T_m^{(AMF)} \simeq 0.68\epsilon_h$. The overall picture thus changes little, with respect to standard mean-field.

In principle, a similar approach can also be implemented within our framework, by considering $H_0$ as a collection of one dimensional Hamiltonian. Analogously to standard spin models, in fact, the one dimensional system can be exactly solved by transfer matrix methods. Indeed, as a simple example of the technique, let us consider in the following an Hamiltonian of the form (we denote with a subscript the site index)

$$H_0 = \sum_r [J\mathrm{S}_r\mathrm{S}_{r+1} + \mathrm{B}\mathrm{S}_r] \tag{2.39}$$

defined on a ring of length $L$ with periodic boundary conditions. The partition function can be written as

$$Z = \mathrm{Tr}\; T(\mathrm{S}_1, \mathrm{S}_2)T(\mathrm{S}_2, \mathrm{S}_3)\ldots T(\mathrm{S}_L, \mathrm{S}_1) \tag{2.40}$$

where $T(\mathbf{S},\mathbf{S}')$ is a transfer matrix of the form

$$T(\mathbf{S},\mathbf{S}') = e^{J\mathbf{S}\mathbf{S}'+\frac{\mathbf{B}\mathbf{S}}{2}+\frac{\mathbf{B}\mathbf{S}'}{2}} \tag{2.41}$$

The free energy per spin in the thermodynamic limit depends only on the largest eigenvalue of $T$. The eigenvalues $\lambda$ and the eigenvector $V(\mathbf{S})$ are determined by the equation

$$\mathrm{tr}_{\mathbf{S}'} T(\mathbf{S},\mathbf{S}')V(\mathbf{S}') = \lambda V(\mathbf{S}) \tag{2.42}$$

where a general form for $V$ is $V(\mathbf{S}) = a + \mathbf{b}\mathbf{S} + (\mathbf{c}\mathbf{S})(\mathbf{c}\mathbf{S})$. After some elementary algebra, we obtain

$$\lambda_{\pm} = \frac{\mathbf{B}^2 + 2J \pm \sqrt{(\mathbf{B}^2+2J)^2 + 8J\mathbf{B}^2}}{4} \tag{2.43}$$

We note that, in particular, the result is correct in two simple limiting cases: when $B = 0$, $Z = J^L$; when $J = 0$, $Z = \left(\frac{\mathbf{B}^2}{2}\right)^L$.

# 3 Phase diagram of a semiflexible polymer chain

In the first chapter we have considered polymers with a chain backbone substantially flexible. This is justified provided that the persistence length $l_p$ is significantly smaller than any other characteristic scales such as the polymer length $L$. On the other hand, several biopolymers (like DNA and actin) appear to be semiflexible, i.e. they have a persistence length that is at least comparable with macroscopic length scales [54].

Considerable theoretical effort has gone into studying the evolution of the coil-globule transition as the stiffness of the polymer is increased (see [55] and references therein). There is indeed some experimental evidence that chain stiffness can affect the character of the collapse transition and even the nature of the collapsed phase [56]. Experiments on polystyrene (a flexible polymer) show a continuous transition from the coil to a liquid-like globule. For DNA molecules (an example of a stiff polymer), a first order transition has instead been observed. The transition takes place between the coil and a compact dense state which has hexagonal order. Some theories [55, 57] predict that the coil-globule transition is second order for flexible polymers but becomes first order as the stiffness increases. However, these theories all assume a liquid-like dense phase and they neglect the possibility of an ordered dense phase.

In this chapter we investigate the effect of local chain stiffness on the collapse transition and, more generally, on the phase diagram of an isolated homopolymer. This will enables us to extend also the studies undertaken in the second chapter, which were restricted to Hamiltonian walks. In the following, indeed, we will include the possibility of both compact and noncompact phases.
Within the framework of a lattice model, the system displays a particularly rich phase behaviour with both first order and second order phase transitions. Our findings support the existence of an open coil at high temperature, a collapse globule at intermediate temperature and low stiffness, and a stretched phase at low temperature and large stiffness. We

also find evidences for a multicritical point.

In paragraph 1 we will describe the lattice model and we will briefly summarize previous results concerning it, mainly those obtained through Monte Carlo simulations [58, 59]. We will also try to make contact with the protein folding problem.
In paragraph 2 we present a discussion of a mean-field approach, originally proposed in [60]. It involves a field theoretical representation of the partition function, which is then evaluated through a saddle point approximation on the functional integral. It is similar in spirit (and it generalizes) a previous approach, which has been used in a series of papers (see [47] and references therein) to derive the phase diagram in the fully compact case.
This analytical treatment, though valuable, turns out to be unsatisfactory in some aspects, so that, in paragraph 3, we are led to the introduction of a novel Bethe approximation [61]. This approach (based on the cluster variation method) constitutes a substantial improvement with respect to mean–field theory, giving results in good agreement with Monte Carlo simulations.
In the last paragraph we discuss a possible scheme to further improve the method according to the cluster variation method.

## 3.1 The model

In this section we present a simple lattice model which incorporates a local stiffness of the chain. We represent a polymer as a self-avoiding walk (SAW) on a $d$-dimensional hypercubic lattice with $V = L^d$ sites. Monomers are placed on the lattice sites and double occupancy of a site is strictly forbidden. The energy of the chain takes into account two contributions. First, a negative energy $-\epsilon_v$ is assigned to each pair of monomers which are unit distance apart and which are not consecutive along the chain. Second, a positive energy $\epsilon_h$ is attributed to each turn (corner) of the walk, i.e. to each pair of successive chain segments which are not collinear. The former is the standard interaction potential of a $\theta$ polymer, the latter models the bending rigidity of the chain. Let $T$ be the absolute temperature and $\beta = \frac{1}{\kappa_B T}$ the inverse temperature. In the following we will adopt the notation $\omega = \beta\epsilon_v$, $t = \frac{T}{\epsilon_v}$ and $x = \frac{\epsilon_h}{\epsilon_v}$. The partition function of the system is

$$Z_N = \sum_{\{S\}} e^{\omega(N_{con}(\mathcal{S}) - xN_{cor}(\mathcal{S}))} \tag{3.1}$$

where $\{S\}$ denotes the ensemble of all $N$–step SAW; $N_{con}(\mathcal{S})$ and $N_{cor}(\mathcal{S})$ are respectively the number of non bonded contacts and corners in walk $\mathcal{S}$. We will find convenient in the following to work in an ensemble where the number of monomer is not fixed but controlled by a chemical potential. Introducing a fugacity $z$ per monomer, the grand canonical partition

function therefore reads

$$\mathcal{Z}(z) = \sum_{N=1}^{\infty} z^N Z_N \tag{3.2}$$

where the sum is over all possible lengths $N$ of the walk. The average number of monomer is given by

$$\langle N \rangle = z \frac{\partial \ln \mathcal{Z}(z)}{\partial z} \tag{3.3}$$

The lattice model (3.1) has been investigated through Monte Carlo simulations by Kolinsky et al. [62, 63]. They focused in particular on the importance of local chain stiffness on the collapse transition of a single polymer. They found evidences that, broadly speaking, polymers can be grouped into two classes, loosely referred to as flexible and stiff. The different qualitative behaviour is controlled by the relative strength of the attractive interaction over the bending energy. Flexible polymers undergo a continuous phase transition from a high-temperature, extended random coil to a low-temperature, compact random globule. This is caused by the attractive interactions between non-bonded units. As the temperature decreases the polymer gradually becomes denser and less extended. Stiff polymers, on the other hand, exhibit a first order phase transition to a dense phase with orientational order. This occurs because the freezing out of the rotational degrees of freedom dominates over the attractive interactions. The system develops a sequence of straight segments with a minimum number of corners.
The authors, though, were not able to go beyond a semi-qualitative interpretation. In particular they could not conclude wether what they observed was a finite-size effect or true asymptotic behaviour.

More recently Bastolla et al. [58] and Doye et al. [59] have performed new, extensive Monte Carlo simulations of the model (3.1). These investigations have been based on two distinct numerical algorithms and the reported results are consistent with each other. The work in [58] has focused on the accurate mapping of the phase diagram, whereas that in [59] has paid special attention to the structural changes of the polymer (especially to the folded structures that form at low temperatures). We report in figure 3.1 the phase diagram obtained in [58] as a function of $x$ and $t$. A similar phase behaviour was observed in [59] . We briefly comment on the figure. The coil-globule transition is second order and it has all typical features of a $\theta$ collapse. The collapse temperature $t_\theta$ is a weakly increasing function of $x$. The melting transition toward the solid ('folded') phase is, instead, first order. The solid phase denotes the anisotropic ordered phase. It is a quasi-frozen phase, with the links of the walk predominantly stretched along one direction of the lattice. The melting temperature $t_m$ increases with $x$ and approximately at $x_c \simeq 13$ it reaches the coil-globule transition

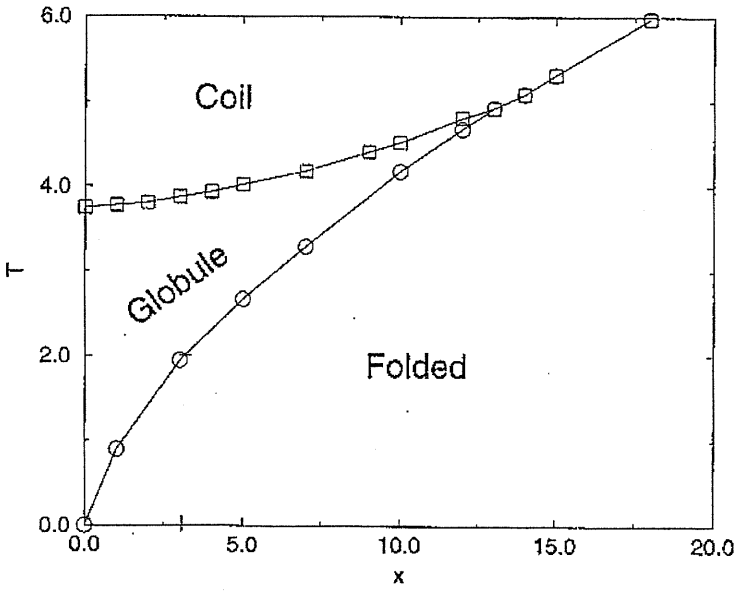


Figure 3.1: Phase diagram of the semiflexible polymer, as obtained from Monte Carlo simulations (from [58]). The 'Folded' state stands for the phase denoted as 'solid' in the text.

temperature. For sufficiently stiff polymers, the disordered globule desappears and there is a direct first order transition from the random coil to the ordered state. Simulations have been performed up to $x = 18$. The melting temperature seems to grow with $x$ and it does not show to attain any asymptotic finite value.

Besides being of clear interest for the melting or crystallization of semiflexible polymers, the present model can be seen as a rudimentary model for proteins. It describes, in a highly simplified way, the formation of secondary structures in globular proteins, although, of course, it lacks of an essential ingredient such as heterogeneity. The connection with the protein folding problem was already suggested by Kolinsky [63] and subsequently reformulated in [60]. It explains part of the recent interest in the model [58, 59, 60, 61]. In this perspective, each link of the walk represents an $\alpha$–helical turn (ca. 3 amino acids). The curvature term mimics the tendency to form local order with one-dimensional character (secondary structures). Indeed, hydrogen bonds have the tendency to favour long helices, that is to align the links of our model. The attractive energy $\epsilon_v$, instead, models the effect of average hydrophobicity, which is supposed to be the main driving force for the folding transition. With this identification, the liquid, compact phase corresponds to the molten globule phase of proteins, whereas the swollen coil is related to the fully unfolded state. The melting transition toward a small entropy crystalline state is the (qualitative) analogous of the folding transition toward the unique native state of a protein. Although one should

be cautious to extend results obtained in the thermodynamic limit to a protein consisting of 100 monomers, the phase behaviour of a semiflexible homopolymer appears to be qualitatively similar to that of a protein. There are in fact two different pathways to go from the denaturated coil state to the native state: either through a direct first order folding transition or through an intermediate liquid globule.

## 3.2 Mean field theory

We sketch in this section the main points of a mean field calculation due to Doniach et al. [60] for the semiflexible model (3.1). It extends a previous approach [47] to the presence of vacancies and to a finite attractive energy between monomers. It therefore enables to include the high temperature disordered state in the phase diagram.

Following the discussion in the previous chapter, we represent the grand partition function (3.2) by means of spin variables. Besides an $n$-component vector $\mathbf{S}_\alpha(\mathbf{r})$, introduced on each lattice site $\mathbf{r}$ and for each direction $\alpha = 1, \ldots, d$, we have to consider a variable $n_\mathbf{r} = 0, 1$. This variable keeps track of the occupation number of lattice site $\mathbf{r}$. We write

$$\mathcal{Z}(z) = \lim_{n\to 0} \frac{1}{n} \left[ \mathrm{Tr} \prod_{\mathbf{r},\alpha} \left[1 + z\mathrm{e}^{-\omega} \mathbf{S}_\alpha(\mathbf{r}) \mathbf{S}_\alpha(\mathbf{r}+\hat{\alpha})\right] \mathrm{e}^{\frac{\omega}{2} \sum_{\mathbf{r},\mathbf{r}'} n_\mathbf{r} \Delta_{\mathbf{r}\mathbf{r}'} n_{\mathbf{r}'}} - 1 \right] \tag{3.4}$$

where $\Delta_{\mathbf{r},\mathbf{r}'} = 1$ if $\mathbf{r}$ and $\mathbf{r}'$ are nearest-neighbours on the lattice, 0 otherwise. The factor $\mathrm{e}^{-\omega}$ in the product ensures that we do not count the attractive energy between consecutive monomers; $z$ represents the monomer fugacity. The trace operation on the spin variables is defined as

$$\langle S_\alpha^i S_\beta^j \rangle = \delta_{ij} \begin{cases} \mathrm{e}^{-\omega x} & \alpha \neq \beta \\ 1 & \alpha = \beta \end{cases} \tag{3.5}$$

$$\langle 1 \rangle = 1 \tag{3.6}$$

and it is zero otherwise. The configuration with all empty bonds (all bond variable equal to 1) is counterbalanced by the factor $-1$ in (3.4). As the variables $\mathbf{S}_\alpha(\mathbf{r})$ and $n_\mathbf{r}$ are not indipendent, it is more convenient to perform an Hubbard-Stratanovich transformation similar to that considered in chapter 2. With a bit of work, the expression (3.4) can be reformulated as

$$\mathcal{Z}(z) = \lim_{n\to 0} \frac{1}{n} \left[ \int \prod_\mathbf{r} d\psi_\mathbf{r} \prod_\alpha d\varphi_\alpha(\mathbf{r}) \mathrm{e}^{-A_G} \prod_\mathbf{r} \left[1 + z\mathrm{e}^{-\omega} \mathrm{e}^{\sqrt{\omega}\psi_\mathbf{r}} B_\mathbf{r}\right] - 1 \right] \tag{3.7}$$

with

$$A_G = \frac{1}{2} \sum_{\mathbf{r},\mathbf{r}'} \psi_\mathbf{r} (\Delta_{\mathbf{r}\mathbf{r}'})^{-1} \psi_{\mathbf{r}'} + \frac{1}{2} \sum_{\alpha=1}^{d} \sum_{\mathbf{r},\mathbf{r}'} \varphi_\alpha(\mathbf{r}) (\Delta^\alpha_{\mathbf{r}\mathbf{r}'})^{-1} \varphi_\alpha(\mathbf{r}') \tag{3.8}$$

and

$$B_{\mathbf{r}} = \frac{1}{2}\left[\sum_{\alpha}\varphi_{\alpha}^{2}(\mathbf{r}) + \mathrm{e}^{-\omega}\sum_{\alpha\neq\beta}\varphi_{\alpha}(\mathbf{r})\varphi_{\beta}(\mathbf{r})\right] \tag{3.9}$$

In equations (3.7), $\varphi_{\alpha}(\mathbf{r})$ and $\psi_{\mathbf{r}}$ are respectively an $n$-component field (needed to perform the transformation on $\mathbf{S}_{\alpha}$) and a scalar field (needed for $n_{\mathbf{r}}$).

We evaluation equation (3.7) through a saddle-point approximation. In the homogeneous and isotropic case, assuming periodic boundary conditions, equation (3.7) specializes to

$$\mathcal{Z}(z) = \lim_{n\to 0}\frac{1}{n}V\left[-\frac{1}{2}\left(\frac{1}{2d}\psi^{2} + \frac{d}{2}\varphi^{2}\right) + \ln\left(1 + z\mathrm{e}^{-\omega}\mathrm{e}^{\sqrt{\omega}\psi}B\right)\right] \tag{3.10}$$

We look for solutions of the form $\vec{\varphi} \propto (1,\ldots,1)$ and $\psi \propto \sqrt{n}$, due to the $1/n$ factor. The saddle-point equations than read

$$\frac{\psi}{2d} = \frac{d\varphi^{2}}{2}\frac{z\sqrt{\omega}\mathrm{e}^{-\omega}\mathrm{e}^{\sqrt{\omega}\psi}\left(1+(d-1)\mathrm{e}^{-\omega}\right)}{D} \tag{3.11}$$

$$\frac{d\varphi}{2} = (d\varphi)\frac{z\mathrm{e}^{-\omega}\mathrm{e}^{\sqrt{\omega}\psi}\left(1+(d-1)\mathrm{e}^{-\omega}\right)}{D} \tag{3.12}$$

with

$$D = 1 + \frac{d\varphi^{2}}{2}z\mathrm{e}^{-\omega}\mathrm{e}^{\sqrt{\omega}\psi}\left(1+(d-1)\mathrm{e}^{-\omega}\right) \tag{3.13}$$

Equation (3.3) in turn gives

$$N = V\frac{d\varphi^{2}}{2}\frac{z\mathrm{e}^{-\omega}\mathrm{e}^{\sqrt{\omega}\psi}\left(1+(d-1)\mathrm{e}^{-\omega}\right)}{D} \tag{3.14}$$

Introducing the monomer density $\rho = N/V$, we obtain

$$\varphi^{2} = \frac{4}{d}\rho \tag{3.15}$$

$$\psi = 2d\sqrt{\omega}\rho \tag{3.16}$$

$$D = \frac{1}{(1-\rho)} \tag{3.17}$$

leading to a free energy per monomer (in unit of $\epsilon_v$)

$$f = -\frac{t}{N}\ln\left(\frac{\mathcal{Z}(z)}{z^{N}}\right) \tag{3.18}$$

$$= -t\ln\left(\frac{q(x/t)}{\mathrm{e}}\right) + t\frac{1-\rho}{\rho}\ln(1-\rho) + 1 - d\rho \tag{3.19}$$

whith

$$q(x/t) = 2 + 2(d-1)\mathrm{e}^{-x/t} \tag{3.20}$$

The high-temperature coil phase corresponds to the limit $\rho \to 0$, whereas space filling Hamiltonian walks are recovered for $\rho = 1$.

As discussed in Chapter 2 the ground state of the system is a compact phase, consisting of straight paths which make turn on the surface of the lattice. In the limit $N \to \infty$, each monomer is surrounded by exactly $2(d-1)$ neighbors. As a consequence, its free energy per monomer is

$$g = -(d-1) \tag{3.21}$$

This phase is not obtained from the saddle point approximation but it is included *ad hoc* in the analysis, as it is expected to exhist.

The phase diagram of the system results by comparing the free energies per monomer $f(\rho)$ and $g$. Above the $\theta$ temperature $t_\theta = 2d$, the free energy is minimized at the extremal point $\rho = 0$. The $\theta$ collapse transition appears to be independent of $x$. It is signalled by a stable phase with non zero density $\rho^*$, which starts to develop at $t_\theta$. The density $\rho^*$ satisfies $\left(\frac{\partial f}{\partial \rho}\right)_{\rho=\rho^*} = 0$, i.e. it is a solution of the equation

$$\frac{\ln(1-\rho^*)}{\rho^*} + 1 + \rho^* \frac{d}{t} = 0 \tag{3.22}$$

A first order melting transition from a disordered globule to an ordered phase should instead occur at $g = f(\rho^*)$. It is interesting to note that, in the limit $x, t \to 0$, the density $\rho^* = 1$ and the results of chapter 2 are recovered. The complete phase diagram as obtained within this framework is reported in figure 3.2.

In the limit $x \to \infty$ the melting temperature is $t_m = d/(4\ln 2 - 2)$. Mean field theory therefore predicts that $t_m < t_\theta$ for any value of $x$ (and in any dimensions) so that it is not possible to obtain a direct transition from the high temperature phase to the crystalline ground state. This is essentially a consequence of two clear drawbacks of the treatment. The first one is that mean field theory provides a rough estimate of the collapse transition. This is not surprising if one considers that the $\theta$ transition is a second order phase transition. As observed in [60], it is possible to improve on this point by using the numerical estimates for $t_\theta$ at $x = 0$. In analogy with mean field theory one then extends this value to the case $x \neq 0$, by assuming that $t_\theta$ does not depend on $x$. In three dimensions, for instance, $t_\theta \simeq 3.64$, whereas the mean field value is $t_\theta = 6$. The phase diagram (3.2) is accordingly modified. For $x > x_c$ ($x_c \simeq 15$) the melting transition occurs at a higher temperature than the $\theta$ collapse and the globular phase dissapears.

The second, and more serious, drawback of the description is related to the finite asymptotic value of the melting temperature $t_m$. This picture is indeed contradicted by Monte Carlo simulations [58, 59] and heuristic arguments [59] which instead suggest that $t_m$ increases indefinetly with $x$. As the $\theta$ temperature has only a small increase with $x$, this leads to the existence of a multicritical point in the phase diagram.

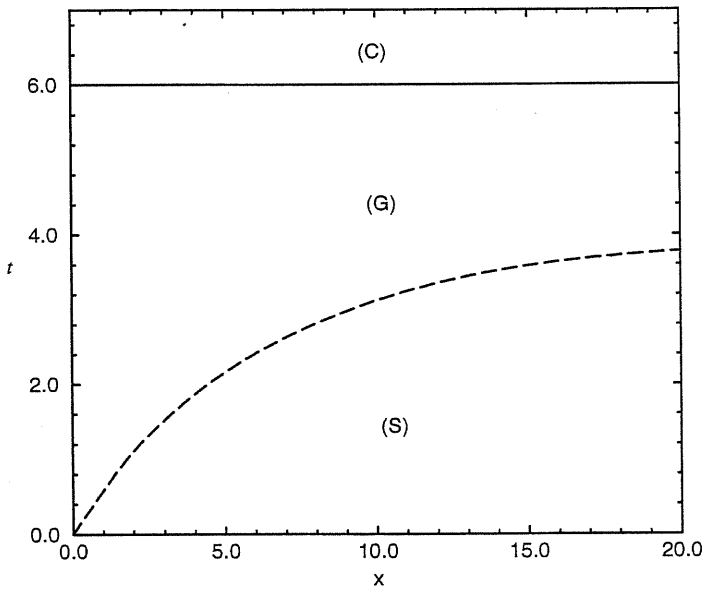


Figure 3.2: Mean field phase diagram of the semiflexible polymer in $d = 3$ (as obtained in [60]). The solid line denotes the continuous $\theta$ transition from the coil (C) to the liquid (G). The dashed line denotes the first order transition to the solid phase (S).

## 3.3 Bethe approximation

As discussed in the previous section, mean field theory is not fully satisfactory. In order to improve it, in this section we will present a Bethe approximation for lattice models of linear homopolymers [61]. We will apply it to study the phase diagram of the semi-flexible chain model, as a function of $t = \frac{T}{\epsilon_v}$ and $x = \frac{\epsilon_h}{\epsilon_v}$.

In the approach to the problem we will follow the cluster variation method (CVM) [64, 65, 66, 67]. This is a closed form approximation, which is known to give excellent results for the phase diagram of spin systems [68]. The approximation scheme is determined by the largest clusters of sites which are treated exactly. The CVM allows to write an approximate expression for the free energy of the system, as a function of the probability of occurrence of all possible configurations of the basic cluster. This free energy has then to be minimized, subject to consistency conditions on the distribution variables. The pair approximation considers nearest-neighbor pair of lattice sites and it corresponds to the Bethe approximation.

In appendix 2 we review for completeness the main ideas about CVM, as formulated by An [67]. This formulation derives the CVM in a very elegant way, directly from the variational principle of statistical mechanics. It turns out to be a particularly convenient starting

point also for our analysis, providing an approximate expression for the entropy $S$ of the system. In the pair approximation, for instance

$$-\frac{S}{N} = \frac{q}{2}\sum_i p_i \ln p_i + (1-q)\sum_i s_i \ln s_i \tag{3.23}$$

where $p_i$ and $s_i$ are the distributions variables assigned respectively to each bond and site configurations ($q$ is the coordination number of the lattice).

Before discussing the results concerning the phase diagram of the semi flexible model (3.1), we illustrate the method by treating in some detail two simpler cases with zero stiffness. We first consider the problem of enumerating Hamiltonian walks (HW) on a lattice (section 1). We then extend this case to interacting self-avoiding walks (section 2), i.e we allow the presence of vacancies and we introduce an attractive interaction between monomers. We finally consider the general case in section 3.

### 3.3.1 Enumeration of Hamiltonian walks

We consider HWs on a $d$–dimensional hypercubic lattice, with $N = L^d$ sites and periodic boundary conditions. In the case $x = 0$ each HW is equally weighted and the total number of paths is believed to scale as $\mathcal{N}_{HW} \simeq \mu_H^N$.
In order to evaluate the entropy from (3.23), one should in principle distinguish among all the possible configurations which are not related by symmetry operations. In $d = 2$ there are, for instance, 2 single site[1] and 8 pair independent configurations. By minimizing numerically eq. (3.23) we have verified that in this particular case they can be grouped into a smaller number of non–equivalent classes. In fact the single site probability $s_i$ is independent of the configuration and the pair probability $p_i$ assumes only two values, depending on wether the nearest–neighbor pair is joined directly by the path or not (see figure 3.3). We can therefore denote with $s$ the site probability ($q(q-1)/2$ configurations) and with $p_1$ and $p_2$ respectively the probability associated with an empty bond ($(q-1)^2(q-2)^2/4$ configurations) and an occupied bond ($(q-1)^2$ configurations). Normalization of the distributions implies

$$s = \frac{2}{q(q-1)} \tag{3.24}$$

Moreover, the reduced density probability, obtained as the partial trace over one sites of the pair configurations, must be consistent with the single site ditribution. This condition requires the pair distributions satisfies

$$s = \frac{(q-1)(q-2)}{2} p_1 = (q-1)p_2 \tag{3.25}$$

[1]The path can either make a corner or go straight at a given site

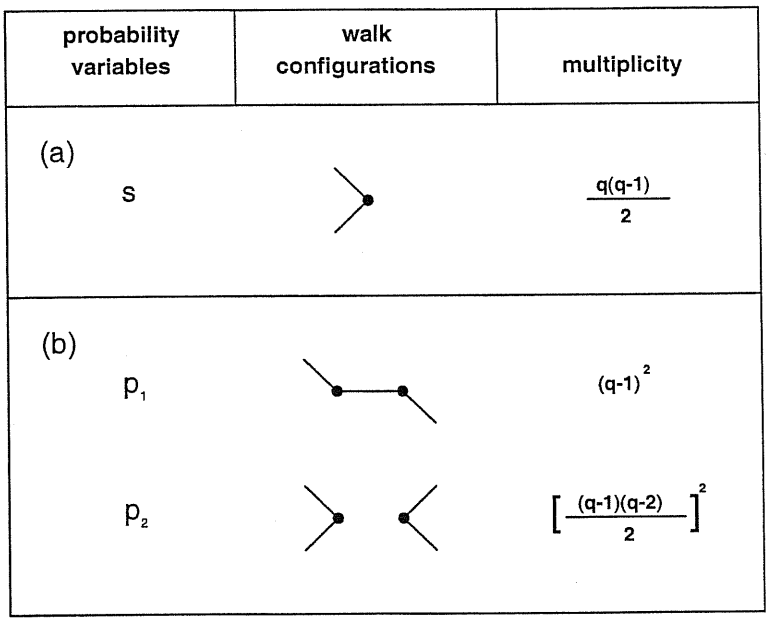


Figure 3.3: Schematic representation of independent (a) site and (b) pair configurations, in the case of Hamiltonian walks. The continuous line represents the path; $q = 2d$ is the coordination number of the lattice.

which together with (3.24) yields

$$p_1 = \frac{4}{q(q-1)^2(q-2)} \tag{3.26}$$

$$p_2 = \frac{2}{q(q-1)^2} \tag{3.27}$$

Substituting (3.24), (3.26) and (3.27) into (3.23), we obtain for the entropy

$$S = \frac{q}{2}\ln(1-\frac{2}{q}) + \ln(\frac{q(q-1)}{(q-2)}) \tag{3.28}$$

This expression coincides with the entropy estimated by using the Flory-Huggins approximation [69]. The latter was originally derived from combinatorial arguments [70]. From (3.28), the connectivity constant in our approximation is thus

$$\mu_H^{(B)} = q\frac{q-1}{q-2}(1-\frac{2}{q})^{\frac{q}{2}} \tag{3.29}$$

In the limit $q \to \infty$, expression (3.29) specializes to

$$\mu_H^{(B)} = \frac{q}{e}(1+\frac{1}{6q^2}+\frac{1}{3q^3}+\ldots) \tag{3.30}$$

The mean field result $\mu_H^{(MF)} = \frac{q}{e}$ is therefore recovered in the limit of infinite coordination. Moreover, by comparing expression (3.30) with the expression (2.27) for $\mu_H$ obtained in the

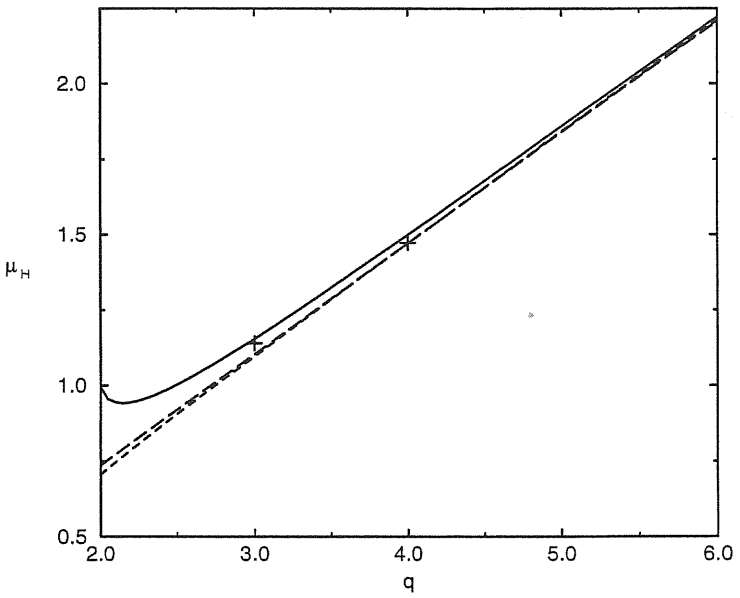


Figure 3.4: The connectivity constant $\mu_H$ as a function of $q$ as obtained from the Bethe approximation (solid line), from the mean field theory (long-dashed line) and by including third-order corrections to mean-field (dashed line). Exact and numerical estimates are drawn with crosses.

previous chapter, we see that the Bethe approximation correctly reproduces the corrections around mean field up to order $O(\frac{1}{q^2})$. In figure 3.4 we report $\mu_H$ as a function of $q$ as obtained from the Bethe approximation, from the mean field theory and by including third-order corrections to mean-field. It is interesting to note that expression (3.29) correctly predicts $\mu_H = 1$ for $d = 1$, contrary to the mean field approximation.

It should be enphasized that the relatively semplicity of the previous calculation is a peculiarity of the pair approximation for the hypercubic lattice. The Bethe approximation for the triangular lattice, for example, does not allow a simple analytical treatment. Indeed the probabilities densities have a more complicated dependence on the configurations of the walk, which results, for instance, in the single site probability taking 3 different values. In this case we obtain numerically $\mu_H \simeq 2.01$ to be compared with the mean–field result $\mu_H \simeq 2.21$. Contrary to the mean-field approximation therefore, the Bethe approximation distinguishes between the cubic and the triangular lattices.

### 3.3.2 Interacting self-avoiding walks

In this section we extend the method, by relaxing the space filling constraint. We also introduce an attractive energy between (non bonded) nearest-neighbour monomers. In this

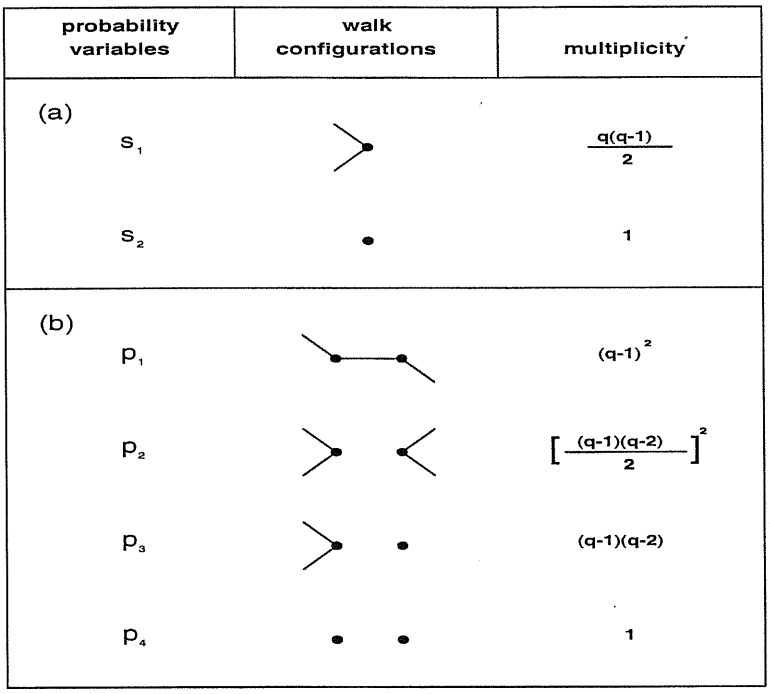


Figure 3.5: Schematic representation of independent (a) site and (b) pair configurations, in the case of SAW. The continuous line represents the path visiting a site; $q = 2d$ is the coordination number of the lattice.

case, in $d = 2$ there are 3 single site and 11 configurations which are not geometrically equivalent. In fact we have to include the possibility of vacancies (empty sites). As for the HW problem of the previous section, it is not necessary to distinguish among all them. They fall into a smaller number of equivalence classes. These are determined only by the following conditions: (a) the site is visited by the path, (b) the nearest–neighbor pair is joined directly by the path. The independent configurations are reported schematically in fig. 3.5, together with their multiplicity of occurrence. Following the notation of fig. 3.5, the free energy of the system (3.2), in the pair approximation, can be written

$$\begin{aligned} \frac{\beta F}{V} &= -\frac{q(q-1)}{2}\ln z s_1 - \frac{q(q-1)^2(q-2)^2}{8}\omega p_2 + \\ &\quad (1-q)\left(\sum_{i=1}^{2} m_s(i) s_i \ln s_i\right) + \frac{q}{2}\left(\sum_{i=1}^{4} m_p(i) p_i \ln p_i\right) \end{aligned} \tag{3.31}$$

where $q = 2d$ is the coordination number of the lattice and $m_s(i)$ and $m_p(i)$ stand respectively for the multiplicity of site and pair configurations. Normalization of the distributions and consistency conditions on the probability variables require respectively

$$s_2 = 1 - \frac{q(q-1)}{2} s_1 \tag{3.32}$$

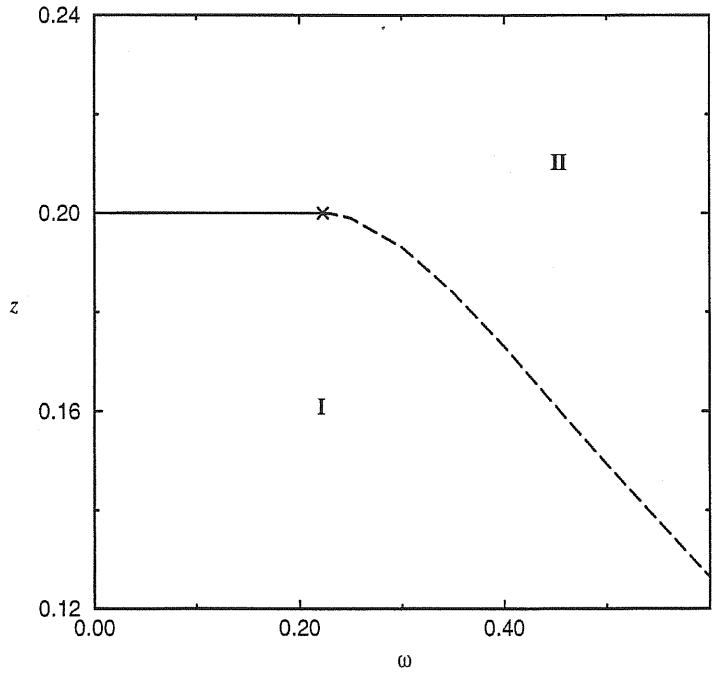


Figure 3.6: Phase diagram of the system as a function of $\omega$ and $z$, in the case of interacting SAW. The average length of the polymer is finite (infinite) in region I (II). The continuous (dashed) line is a second (first) order transition. The cross marks the tricritical point ($\omega_\theta \approx 0.2231$ and $z_\theta = 0.2$).

and

$$\begin{aligned} p_1 &= \frac{s_1}{(q-1)} \\ p_2 &= \frac{2s_1}{(q-1)(q-2)} - \frac{2}{(q-1)(q-2)}p_3 \\ p_4 &= 1 - \frac{q(q-1)}{2}s_1 - \frac{(q-1)(q-2)}{2}p_3 \end{aligned} \tag{3.33}$$

Contrary to the HW case, after substitution of (3.32) and (3.33) into (3.31), we are still left with two undetermined, variational parameters, e.g. $s_1$ and $p_3$. The stable phase at a given $z$ and $\omega$ is determined by minimizing (3.31) with respect to $s_1$ and $p_3$. We report the complete phase diagram for $d = 3$ in fig. 3.6. The polymer is a critical system along the transition line $z_c(\omega)$. This line separates a chain with zero density ($s_1 = 0$ for $z < z_c(\omega)$) from a chain with finite density ($s_1 \neq 0$ for $z > z_c(\omega)$). The continuous line represents a second order transition and the average number of monomers diverges with a power law as $z$ tends to $z_c$. The broken line is instead a first order transition and the density of monomers makes a finite jump at $z_c$. The cross denotes the tricritical point and it corresponds to the $\theta$ point. In the case of pure SAW ($\omega = 0$) the connectivity constant is $\mu = z_c^{-1} = 2d - 1$.

This result would have been expected by studying SAW on a Bethe lattice and it should be compared, for instance, with $\mu \approx 2.64$ [12] and $\mu \approx 4.68$ [14], obtained from exact enumerations respectively in $d = 2$ and $d = 3$.

In our framework $z_c$ does not depend on $\omega$, as long as $\omega < \omega_\theta$. This is certainly an artifact of the approximation, which can be ascribed to the following consideration. After minimization of the free energy (3.31) with respect to $p_3$ we obtain the condition

$$p_3 = \left(\frac{p_2 p_4}{e^\omega}\right)^{\frac{1}{2}} \tag{3.34}$$

We are interested in the case $s_1 \to 0$ since in the proximity of a second order transition line the minimum of the free energy shifts continuously from $s_1 = 0$ to a non zero value. Substituting expressions (3.33) for $p_2$ and $p_4$ into (3.34), we obtain in this limit

$$p_3 \sim s_1 + O(s_1^2) \tag{3.35}$$

As a consequence, from (3.33), $p_2 \sim O(s_1^2)$. The critical $z_c$ is signalled by a change of sign in the derivative of the free energy (3.31) $\partial F/\partial s_1$, evaluate at $s_1 = 0$. As $\omega$ does not contribute to this term, $z_c$ is constant. Nonetheless the estimates we obtain for the $\theta$ point $\omega_\theta^{(B)}$ are a better approximation to the available numerical values, with respect to mean field theory ($\omega_\theta^{(MF)} = \frac{1}{2d}$): in $d = 2$, $\omega_\theta \approx 0.665$[15], $\omega_\theta^{(B)} \approx 0.4055$ and $\omega_\theta^{(MF)} = 0.25$; in $d = 3$, $\omega_\theta \approx 0.275$[16], $\omega_\theta^{(B)} \approx 0.2231$ and $\omega_\theta^{(MF)} = 0.1667$.

### 3.3.3 The semiflexible model

Following the discussion of previous sections, we now generalize the treatment to the case of finite stiffness ($x \neq 0$). Because of the curvature energy, the weight of a configuration depends on the number of corners. Moreover the spatial directions are not a priori all equivalent as we have to include the possibility of an anisotropic phase. On a square lattice, for instance, the ground state of the system consists of a series of parallel segments with corners at the surface of the lattice. For this reason we have to distinguish between one 'special' (named 'horizontal' in the following) direction and the remaining $d-1$ ('vertical') directions. Because of these considerations, it is clearly not possible to group configurations into a small set of classes, as done in the previous two sections. In two dimensions, there are, for example, 11 horizontal and 11 vertical indipendent pair configurations (see figure 3.8) and these numbers increase with spatial dimensionality. We report the 5 indipendent single site configurations in figure 3.7. For clarity, we show only the indipendent pair configurations for $d = 2$ in figure 3.8. We denote with $h_i$ and $v_i$ respectively the horizontal and vertical configurations.

The free energy of the system can be written as a function $s_i$, $h_i$ and $v_i$ in complete analogy

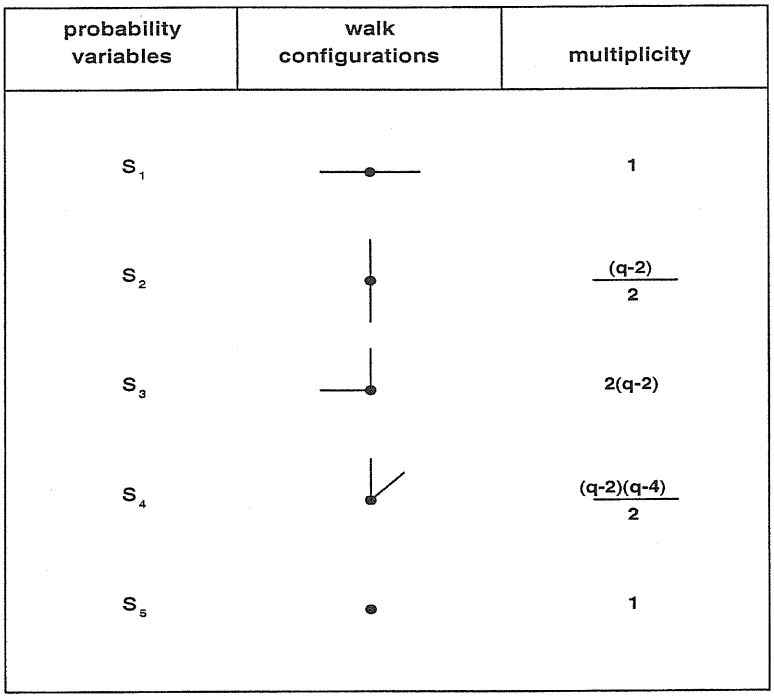


Figure 3.7: Schematic representation of independent single site configurations, in the case of a semiflexible chain.

to the HW and the SAW cases. The task of determining its local minima is instead more complex. It is even further complicated by the inclusion of a number of constraints that the density probabilities must satisfy. An efficient way of doing it numerically is by means of the natural iteration method (NIM), introduced to Kikuchi [65, 66]. This is an iterative alghoritm which is able to solve minimazition problems involving Lagrange multipliers (for details see also the application in [71, 72]). The resulting phase diagram is reported in figure 3.9, as a function of $x$ and $t$ for $d = 3$. The fugacity $z$ is fixed to its critical value $z_c(x,t)$. This condition assures we are studying a polymer in the limit of infinite chain length ($N \to \infty$). We find three different phases: an open coil, a compact globule and an ordered crystal. In our approximation, the latter is just the ground state of the polymer, having all links perfectly aligned. This is known to be not completely correct, as it has been shown rigorously that, for instance, in the case of Hamiltonian walks the entropy strictly vanishes only in the limit $T \to 0$ [73, 74]. The $\theta$–collapse line between the coil and the globule is a second order phase transition and it appears to be independent of $x$. On the other hand the discontinuous melting transition tends to infinity with $x$. Beyond the triple point at $x \simeq 8.8$, there is directly a first order transition from the coil to the solid.

In the limit $T \to 0$ (or $z \to \infty$) we recover the Flory model of polymer melting (see

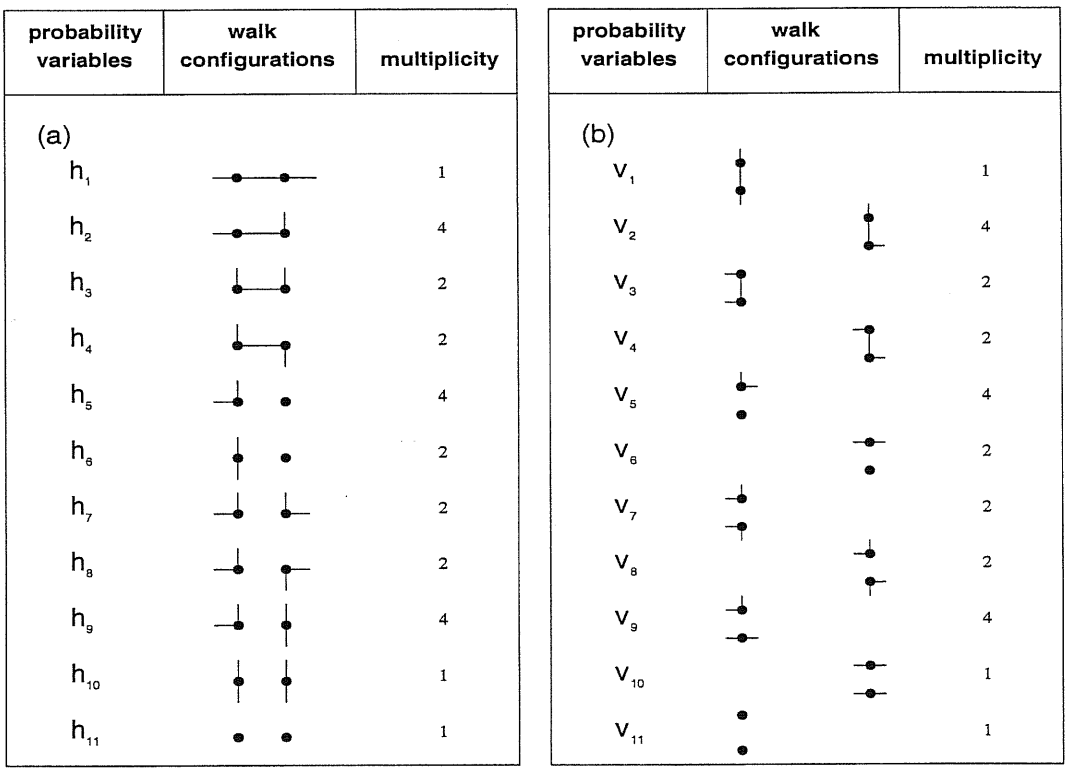


Figure 3.8: Schematic representation of (a) horizontal and (b) vertical pair configurations, in the case of a semiflexible chain in $d = 2$.

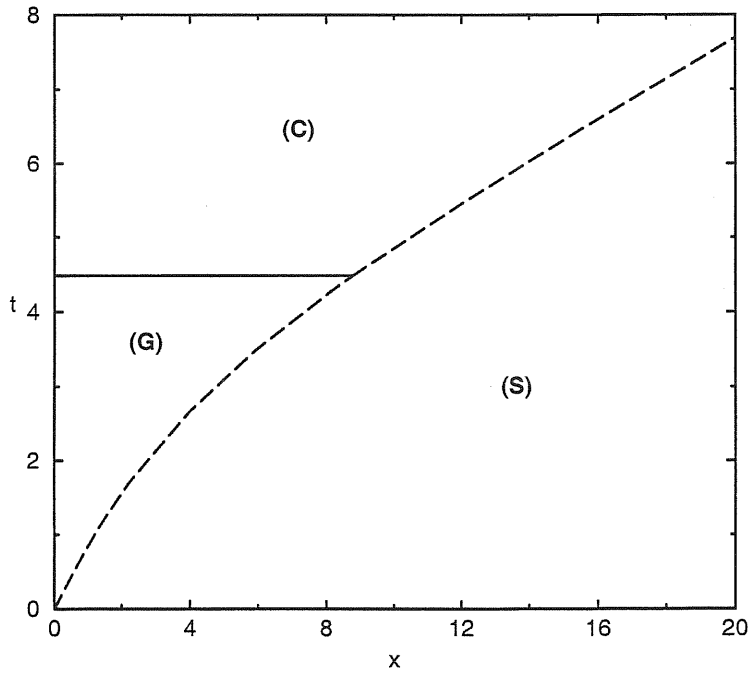


Figure 3.9: Phase diagram of the semiflexible model in $d = 3$ as a function of $x$ and $t$. The continuous line denotes the $\theta$ transition from the coil (C) to the globule (G). The dashed line represents the first order transition to the solid (S). The triple point is at $x \approx 8.8$ and $t \approx 4.5$.

chapter 2). In this limit, walks are space filling and configurations with vacancies do not contribute to the partition function (3.2). Also, the attractive nearest–neighbor potential $\epsilon_v$ plays no role as there are precisely $(d-1)$ contacts per monomer. Similarly to the problem of enumerating HW, we obtain a minimum for the free energy in the disordered, compact phase which coincides with the free energy estimated by using the Flory-Huggins approximation [69]. Neglecting the constant contribution proportional to $\epsilon_v$, the analytical expression reads

$$\frac{\beta F_{FH}}{V} = \ln\left[\frac{\left(1-\frac{2}{q}\right)^{-\left(\frac{q}{2}-1\right)}}{1+(q-2)\exp\left(-\omega x\right)}\right] \tag{3.36}$$

At low temperature $F_{FH}$ competes for stability with the local minimum associated to the ordered phase, which has strictly $F_O = 0$ in our approach. A first order phase transition takes therefore place at

$$t_m = \frac{x}{\ln\left[\frac{q-2}{\left(1-\frac{2}{q}\right)^{-\left(\frac{q}{2}-1\right)}-1}\right]} \tag{3.37}$$

In particular for $d=3$ $(q=6)$ we have $t_m/x = \left(\ln\left(\frac{16}{5}\right)\right)^{-1} \approx 0.86$, which corresponds to the slope of the globule-solid transition line of fig. 3.9, in the limit $x \to 0$. This value is slightly larger than the analogous mean-field estimate, $t_m/x \approx 0.58$.

## 3.4 Plaquette approximation

It is clear that a CVM approximation is uniquely defined by the choice of the maximal clusters and for this reason one speaks of the plaquette approximation, the cube approximation and so on. As a rough rule of the thumb, in the case of discrete spin systems, the accuracy of the approximation improves by taking larger and larger basic clusters.
The pair approximation for the semiflexible polymer gives satisfactory results but it still includes some inaccurate features. For instance, for the Flory model it predicts in any dimensions a first order melting transition toward a completely frozen crystalline state. A transfer matrix study in two dimensions by Saleur [75] shows instead the existence of a continuos transition from a disordered state to a partially ordered phase.

In an attempt to correct these aspects we consider in the following the plaquette approximation on a square lattice. Denoting with $E_i$ the energy associated the $i$-th plaquette configuration, the free energy of the system reads

$$\frac{\beta F}{V} = \beta \sum_i E_i u_i + \left(\sum_i s_i \ln s_i - \sum_i p_i \ln p_i + \sum_i u_i \ln u_i\right) \tag{3.38}$$

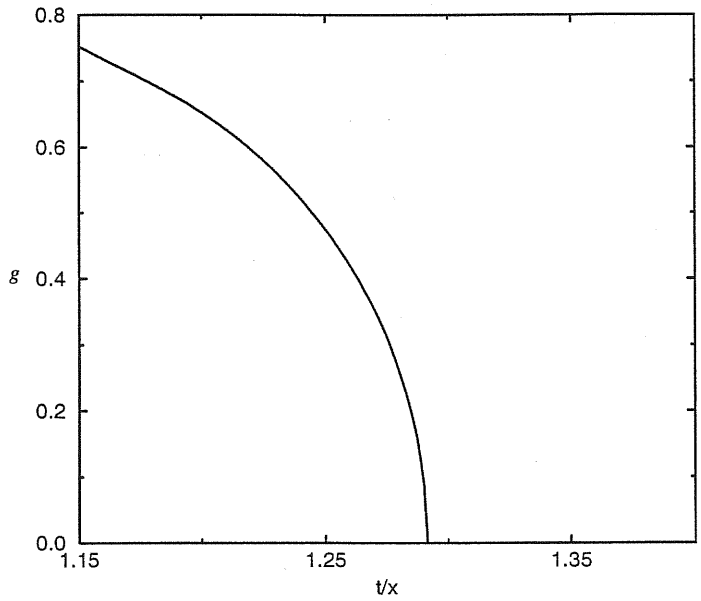


Figure 3.10: Order parameter $g = s_1 - s_2$ for the melting transition of the Flory model, in the case of the plaquette approximation.

where $s_i$ $(i = 1, \ldots, 4)$, $p_i$ $(i = 1, \ldots, 22)$ and $u_i$ $(i = 1, \ldots, 55)$ stand respectively for the distribution variables assigned to each site, bond and plaquette configurations. In the case of the Flory model, we find a second order phase transition at $t_m \simeq 1.29x$. A suitable order parameter for the transition is $g = s_1 - s_2$, where $s_1$ and $s_2$ are the site probabilities associated with a straight path respectively in the horizontal and vertical direction (see figure 3.7). Indeed below the transition point the isotropy of the system is broken and $s_1 \neq s_2$. We show in figure 3.10 the behaviour of $g$ as a function of $t/x$. The estimates for the melting temperature in $d = 2$ as obtained from different approaches are collected in table 3.1.

When $x = 0$ we recover the problem of enumerating HWs on a square lattice. We find $\mu_H \simeq 1.505$ which compares well with the numerical $\mu_H \simeq 1.4728$. Although it does not strictly improve on mean field theory ($\mu_H = 1.5$), it seems to indicate that at least the scheme is 'stable'.

There are instead some difficulties in extending the treatment with the plaquette approximation to the general case. We illustrate them in the case of pure self-avoiding walks ($x = 0$ and $w = 0$). After minimization of the free energy, a correct picture would predict a solution $s_1 = 0$ for $z \leq z_c$ which continuously moves to a solution $s_1 > 0$ as $z > z_c$. In contrast we find a dense polymer phase ($s_1 \neq 0$) for any value of $z > 0$.

The same kind of problem can be recognized to occur even at the lowest order of the ap-

| method | melting temperature |
|---|---|
| mean-field (MF) | 0.98 |
| anisotropic mean-field (AMF) | 1.44 |
| bethe approximation (BA) | 1.44 |
| plaquette approximation (PA) | 1.29 |
| transfer matrix (TM) | 1.55 |

Table 3.1: Numerical values for the melting temperature of the Flory model (in units of the stiffness coefficient $x$) in $d = 2$ as obtained from different approaches. The TM and the PA predict a second order transition, whereas the other methods find a first order transition. The transition occurs at $t_m = (\ln 2)^{-1} x$ both for the AMF and the BA; this is likely to be coincidence.

proximation scheme, where one consider as maximal clusters just the collection of all single sites. This level, in general, corresponds to mean-field theory. Let $p$ be the probability of a site being occupied and $1-p$ the probability of being empty. The free energy of the system is accordingly

$$\frac{\beta F}{V} = -p \ln z + (1-p)\ln(1-p) + p \ln\left(\frac{2p}{q(q-1)}\right) \tag{3.39}$$

This expression is minimized by a non zero $p$ for any finite $z$. The problem can be seen to arise from the term of the form $p \ln p$. In the Bethe approximation these terms exactly cancel for some reason which are not clear at the moment.

# Conclusions

In this thesis we have discussed some models of interacting self-avoiding walks (SAW). In particular, we have focused on investigations motivated by biological applications.

In the first chapter we have studied the collapse of a polymer model which presents an energy frustration due to steric effects. We have determined the phase diagram of the system by performing exact enumerations of SAWs up to 28 steps and through a heuristic argument, based on energy-entropy balance. Such a phase diagram presents a swollen, a compact and a branched phase (BP), in agreement with that of a similar model introduced by Dekeyser et al. [26] . The tricritical line separating the compact and the swollen phase is in the $\theta$ point universality class. The transition between linear and branched polymer is characterized by a critical exponent $\nu_{s-b} \simeq 0.70$, as deduced from series analysis and Monte-Carlo simulations. This value seems to be higher than that obtained in [26]. It disagrees also with an investigation made by Orlandini et al. [76] on a different model who have quoted $\nu_{s-b} = 0.66 \pm 0.03$. The latter model is a two tolerant walk, i.e. a SAW which can visit each bond of the lattice at most twice. By favoring doubly visited bonds with respect to those singly visited, a transition from swollen to BP behavior occurs. More recently, a similar transition has been observed by Orlandini et al. [77] in a hydrophilic-hydrophobic polymer chain, with a periodic distribution of 'charges'[2] along the chain. Using extensive Monte Carlo simulations, they have found an exponent at the transition $\nu_{s-b} \simeq 0.70$, in accordance with our results. The compact-branched phase transition, finally, need more investigations due to a common limitation of series expansion for similar problems [29]. It should be possible to obtain more accurate results with a transfer matrix techniques.
It is important to stress the importance of the square lattice in obtaining a branched polymer phase. In the continuum, or on some other lattices the model (if not suitably modified) might replace this phase with a somewhat loosely packed compact phase.

The model we have investigated can be thought of as an annealed version of an attractive SAW. There are two types of beads: small beads which are allowed to have as many nearest

[2]The 'charge' characterizes the affinity of the monomer for water

neighbors as possible and large beads which allow only one, non bonded, nearest neighbor. The parameter $\epsilon$ plays the role of a fugacity for large beads. An interesting perspective would be to analyze the model in its quenched version where a bead is small with probability $p$ and large with probability $1-p$. In this case it is believed to capture the size effect of different amino acids in the protein folding problem.

In chapter 2 we have investigated Hamiltonian walks (HW) on a regular lattice, starting from a spin representation of the problem which had not be considered before. We have estimated the number of HW on a lattice, using a high-temperature expansion performed at a fixed order parameter. This approach has enabled us to calculate the connectivity constant ($\mu_H$) of HW up to third order in $1/d$. We have found

$$\mu_H = \frac{2d}{e}\left[1 + \frac{1}{24}\frac{1}{d^2} - \frac{1}{12}\frac{1}{d^3} + O(\frac{1}{d^4})\right] \tag{3.40}$$

This result extends of one order previous results, based on a field theoretic representation of the partition function. It is interesting to note that the $1/d^2$ and $1/d^3$ terms exactly cancel for the square lattice, which explains the excellent agreement of the mean field result ($\mu_H^{(MF)} = 1.4715$) with numerical estimates ($\mu_H \simeq 1.4728$).

We have also performed a mean field calculation for HWs with a bending rigidity (the Flory model). In this case our approach (based on the Gibbs-Bogoliubov inequality) coincides with previous saddle point approximations of the partition function. We find a first order transition between a fully stretched phase at low temperature (with zero free energy) and a liquid phase at high temperature. The major drawback of the approach, though, is that the frozen phase is not obtained within the mean field approximation. Its presence is inferred from general thermodynamical considerations, which dictate that the free energy of the model cannot be positive. In addition, it is worth mentioning that, as pointed out by Gujrati and coworkers [73, 74], such a freezing transition cannot be thoroughly correct, since the free energy can be shown to be strictly negative at low temperatures. It might be possible to improve on these points by considering more complex mean-field approximations. For instance, one could consider as a trial Hamiltonian in the variational approach a collection of one dimensional or quasi one-dimensional Hamiltonian. The latter are defined on a ladder structure and are still exactly solvable.

In chapter 3 we have presented a Bethe approximation which is apt to study lattice models of linear homopolymers. The method is based on the cluster variation method and constitutes a substantial improvement with respect to mean–field theory. Indeed, in the case of a semi-flexible polymer chain, it produces a phase diagram with a coil, a globular and a stretched phase, in good agreement with Monte Carlo simulations. In particular, we find a triple point where the $\theta$ collapse line to the globular phase and the melting transition line to the

anisotropic phase meets, which was not predicted by mean-field theory. For sufficiently stiff polymers, therefore, there is a direct first order transition from the expanded coil to the anisotropic phase. The latter is characterized by global orientational order.
In the limit of Hamiltonian walks we recover results of the Flory-Huggins theory for polymer melting, whose variational nature appears in a transparent shape within our framework. The melting temperature is

$$t_m = \frac{x}{\ln\left[\frac{2d-2}{\left(1-\frac{1}{d}\right)^{-(d-1)}-1}\right]} \tag{3.41}$$

which is larger than the corresponding mean-field estimate. In the case of non-weighted HWs, we obtain for the connectivity constant $\mu_H$

$$\mu_H = d\frac{2d-1}{d-1}\left(1-\frac{1}{d}\right)^d \tag{3.42}$$

The mean-field result is recovered in the limit of infinite coordination and corrections to it are reproduced up to second order in $1/d$.
The method has the advantage of not requiring any spin or field theoretical representation, rather it relies directly on the configurations of the system. This last consideration suggests that the scheme is more general and suitable to be applied to other geometrical problems, as, for instance, branched polymers and self-avoiding surfaces (see [5] and references therein). Moreover, contrary to mean field theory, the phase behavior of the system is obtained without any ad hoc assumption on the nature of the phases. It is plausible that the accuracy of the method can be systematically refined according to the cluster variation method, in analogy with spin systems. We expect some of the inaccurate features of the pair approximation could be removed by considering larger basic clusters, although we have not yet been able to devise a general scheme.

# Appendix A
# High temperature expansion of the magnetization dependent free energy

In [50] Georges and Yedidia have presented a formalism for computing the high temperature expansion of the magnetization dependent free energy in the case of the Ising model. In this appendix we extend it to a general $O(n)$ model and to the peculiar trace operation involved in the Hamiltonian walks formalism (see chapter 2).

We consider an Hamiltonian of the form

$$H = -\sum_{ij} J_{ij} \mathbf{S}_i \mathbf{S}_j \tag{A.1}$$

where $\mathbf{S}_i$ is an $n$-components spin vector defined at site $i$. The corresponding partition function in presence of an external magnetic field is

$$Z = \mathrm{Tr}\ \exp\left[-\beta H + \sum_i \lambda_i \mathbf{S}_i\right] \tag{A.2}$$

where Tr is a suitable trace operation over the $\mathbf{S}$ variables. The thermal expectation value of an operator $O$ is evaluated as

$$\langle O \rangle \equiv \frac{\mathrm{Tr}\ O \exp\left[-\beta H + \sum_i \lambda_i \mathbf{S}_i\right]}{Z} \tag{A.3}$$

The magnetization dependent free energy (Gibbs potential) is given by

$$-\beta A = \ln \mathrm{Tr}\ \exp\left[-\beta H + \sum_i \lambda_i (\mathbf{S}_i - \mathbf{m}_i)\right] \tag{A.4}$$

The Lagrange multipliers $\lambda_i(\beta)$ are $n$-components vectors and fix the magnetization at each site $i$ to the average value $\mathbf{m}_i \equiv \langle \mathbf{S}_i \rangle$ (indipendent of $\beta$). They satisfy the following

thermodynamic relation

$$\lambda_i = \frac{\partial \beta A}{\partial \mathbf{m}_i} \tag{A.5}$$

We define an operator $U$ as follows

$$U \equiv H - \langle H \rangle - \sum_i \frac{\partial \lambda_i(\beta)}{\partial \beta}(\mathbf{S}_i - \mathbf{m}_i) \tag{A.6}$$

The derivative of the expectation value of an operator $O$ is given by

$$\frac{\partial \langle O(\beta) \rangle}{\partial \beta} = \langle \frac{\partial O(\beta)}{\partial \beta} \rangle - \langle OU \rangle \tag{A.7}$$

The fact that the magnetization does not depend on $\beta$ results in some useful identities for $U$. The first is trivial

$$\langle U \rangle = 0 \tag{A.8}$$

Next, using equation (A.7) we find that

$$\frac{\partial \langle \mathbf{S}_i \rangle}{\beta} = -\langle U \mathbf{S}_i \rangle = -\langle U(\mathbf{S}_i - \mathbf{m}_i) \rangle = 0 \tag{A.9}$$

The first derivative of $U$ with respect to $\beta$ is

$$\begin{aligned} \frac{\partial U}{\partial \beta} &= \langle HU \rangle - \sum_i \frac{\partial^2 \lambda_i}{\partial \beta^2}(\mathbf{S}_i - \mathbf{m}_i) \\ &= \langle U^2 \rangle - \sum_i \frac{\partial^2 \lambda_i}{\partial \beta^2}(\mathbf{S}_i - \mathbf{m}_i) \end{aligned} \tag{A.10}$$

The second derivative gives

$$\begin{aligned} \frac{\partial^2 U}{\partial \beta^2} &= 2\langle U \frac{\partial U}{\partial \beta} \rangle - \langle U^3 \rangle - \sum_i \frac{\partial^3 \lambda_i}{\partial \beta^3}(\mathbf{S}_i - \mathbf{m}_i) \\ &= -\langle U^3 \rangle - \sum_i \frac{\partial^3 \lambda_i}{\partial \beta^3}(\mathbf{S}_i - \mathbf{m}_i) \end{aligned} \tag{A.11}$$

As we are interested in a Taylor expansion, we consider now the derivatives of the free energy with respect to $\beta = 0$. The first derivatives is given by

$$\frac{\partial(\beta A)}{\partial \beta} = \langle H \rangle - \sum_i \frac{\partial \lambda_i}{\partial \beta}(\mathbf{S}_i - \mathbf{m}_i) = \langle H \rangle \tag{A.12}$$

Successive derivatives are

$$\frac{\partial^2(\beta A)}{\partial \beta^2} = -\langle HU \rangle = -\langle U^2 \rangle$$

$$
\begin{aligned}
\frac{\partial^3(\beta A)}{\partial\beta^3} &= \langle U^3\rangle - 2\langle U\frac{\partial U}{\partial\beta}\rangle = \langle U^3\rangle \\
\frac{\partial^4(\beta A)}{\partial\beta^4} &= -\langle U^4\rangle + 3\langle U^2\rangle^2 - 3\sum_i \frac{\partial^2\lambda_i}{\partial\beta^2}\langle U^2(\mathbf{S}_i - \mathbf{m}_i)\rangle \qquad \text{(A.13)} \\
\frac{\partial^5(\beta A)}{\partial\beta^5} &= \langle U^5\rangle - 10\langle U^3\rangle\langle U^2\rangle - 3\sum_i \frac{\partial^3\lambda_i}{\partial\beta^3}\langle U^2(\mathbf{S}_i - \mathbf{m}_i)\rangle + 7\sum_i \frac{\partial^2\lambda_i}{\partial\beta^2}\langle U^3(\mathbf{S}_i - \mathbf{m}_i)\rangle \\
&\quad +6\sum_i\sum_j \frac{\partial^2\lambda_i}{\partial\beta^2}\frac{\partial^2\lambda_j}{\partial\beta^2}\langle U(\mathbf{S}_i - \mathbf{m}_i)(\mathbf{S}_j - \mathbf{m}_j)\rangle
\end{aligned}
$$

At $\beta = 0$ the spin-spin correlation functions always factorize, so that the expressions (A.13) simplify. Denoting with a 0 subscript the quantities evaluated at $\beta = 0$, we find

$$\frac{\partial(\beta A)}{\partial\beta} = \langle H\rangle_0 = -\sum_{ij} J_{ij}\mathbf{m}_i\mathbf{m}_j \qquad \text{(A.14)}$$

From equation (A.5) and (A.14) follows

$$\left.\frac{\partial\lambda_i}{\partial\beta}\right|_{\beta=0} = \left.\frac{\partial^2(\beta A)}{\partial\mathbf{m}_i\partial\beta}\right|_{\beta=0} = -\sum_{j(\neq i)} J_{ij}\mathbf{m}_i \qquad \text{(A.15)}$$

Substituting (A.15) into (A.6), we obtain for the operator $U_0$

$$U_0 = -\sum_{ij} J_{ij}(\mathbf{S}_i - \mathbf{m}_i)(\mathbf{S}_j - \mathbf{m}_j) \qquad \text{(A.16)}$$

In order to perform calculations it is often convenient to use a diagramatic notation, which represents the term $(\mathbf{S}_i - \mathbf{m}_i)(\mathbf{S}_j - \mathbf{m}_j)$ by a link.

We now specilize to Hamiltonian walks, so that $J_{ij} = 1$ if site $i$ and $j$ are nearest neighbour on the lattice and zero otherwise. The trace operation moreover satisfies

$$\text{tr } 1 = \text{tr } S_i^\alpha = \text{tr } S_i^{\alpha_1}\ldots S_i^{\alpha_k} = 0 \quad \text{if } k \neq 2 \qquad \text{(A.17)}$$

and

$$\text{tr } S_i^\alpha S_i^\beta = \delta_{\alpha,\beta} \qquad \text{(A.18)}$$

From definitions (A.17) and (A.18) follows

$$\langle (S_i^\alpha - m^\alpha)((S_i^\beta - m^\beta)\rangle = \delta^{\alpha\beta}\frac{\mathbf{m}^2}{2} - m^\alpha m^\beta \qquad \text{(A.19)}$$

$$\langle (S_i^\alpha - m^\alpha)(S_i^\beta - m^\beta)(S_i^\gamma - m^\gamma)\rangle = 2m^\alpha m^\beta m^\gamma - \frac{\mathbf{m}^2}{2}(m^\alpha\delta_{\beta\gamma} + m^\beta\delta_{\alpha\gamma} + m^\gamma\delta_{\alpha\beta}) \qquad \text{(A.20)}$$

and, in the general case,

$$\langle (S_i^{\alpha_1} - m^{\alpha_1}) \ldots (S_i^{\alpha_k} - m^{\alpha_k}) \rangle = (-1)^{k-1} \left( (n-1) m^{\alpha_1} \ldots m^{\alpha_k} - \frac{\mathrm{m}^2}{2} \sum_{\{P\}} \delta_{\alpha_1,\alpha_2} m^{\alpha_3} \ldots m^{\alpha_k} \right) \tag{A.21}$$

where $\{P\}$ denotes a sum over all possible distinct choices of pairs among the $k$ index labels. Using equation (A.13) and (A.21) we can compute

$$\begin{aligned} \frac{\partial^2(\beta A)}{\partial \beta^2} &= -\langle U_0^2 \rangle \\ &= -\sum_{\langle ij \rangle} \sum_{\langle kl \rangle} \langle [(\mathbf{S}_i - \mathbf{m})(\mathbf{S}_j - \mathbf{m})] [(\mathbf{S}_k - \mathbf{m})(\mathbf{S}_l - \mathbf{m})] \rangle \\ &= -\sum_{\langle ij \rangle} \langle [(\mathbf{S}_i - \mathbf{m})(\mathbf{S}_j - \mathbf{m})]^2 \rangle = N d \frac{\mathbf{m}^4}{4} n \end{aligned} \tag{A.22}$$

and

$$\begin{aligned} \frac{\partial^3(\beta A)}{\partial \beta^3} &= \langle U_0^3 \rangle \\ &= -\sum_{\langle ij \rangle} \sum_{\langle kl \rangle} \sum_{\langle pq \rangle} \langle [(\mathbf{S}_i - \mathbf{m})(\mathbf{S}_j - \mathbf{m})] [(\mathbf{S}_k - \mathbf{m})(\mathbf{S}_l - \mathbf{m})] [(\mathbf{S}_p - \mathbf{m})(\mathbf{S}_q - \mathbf{m})] \rangle \\ &= -\sum_{\langle ij \rangle} \langle [(\mathbf{S}_i - \mathbf{m})(\mathbf{S}_j - \mathbf{m})]^3 \rangle = \frac{dN}{2} \mathbf{m}^6 \end{aligned} \tag{A.23}$$

Higher derivatives of $\beta A$ can be obtained by a continuation of these procedures.

# Appendix B
# The cluster variation method

The cluster variation method (CVM) is a closed form approximation scheme, originally introduced by Kikuchi [64] and subsequentially reformulated several times [68]. In the following we briefly review the main idea of the CVM, following the exposition in [67]. We also remand to [71, 72] for a clear illustration and applications of the procedure.

Let $H$ be the Hamiltonian of a model system on a lattice $\Lambda$ and let $\kappa_B$ and $T$ be respectively the Boltzmann's constant and the absolute temperature. The free energy of the system can be obtained by minimizing the functional

$$F[\rho] = \mathrm{Tr}\ (\rho H) + \kappa_B T\,(\mathrm{Tr}\ \rho \ln \rho) \tag{B.1}$$

with respect to $\rho$, subject to the constraint $\mathrm{Tr}\ \rho = 1$. The minimization is achieved at

$$\rho = \frac{\mathrm{e}^{-H/\kappa_B T}}{\mathrm{Tr}\ \mathrm{e}^{-H/\kappa_B T}} \tag{B.2}$$

which gives the density matrix of the system. If the minimization is carried out on a restricted class of functions, one is led to a particular closed-form approximation.

The reduced density matrix for a cluster $\alpha$ consisting of $n_\alpha$ sites is defined as

$$\rho_\alpha = \mathrm{Tr}_{\ \Lambda/\alpha}\rho \tag{B.3}$$

where the partial trace is taken over all variables in $\Lambda$, except those in $\alpha$. The cluster entropy associated with $\rho_\alpha$ is defined via

$$S_\alpha = -\kappa_B \mathrm{Tr}\ \rho_\alpha \ln \rho_\alpha \tag{B.4}$$

which is expanded in cumulants by writing

$$S_\alpha = \sum_{\beta \subseteq \alpha} \tilde{S}_\beta \tag{B.5}$$

It can be shown that

$$\tilde{S}_\beta = \sum_{\alpha \subseteq \beta} (-1)^{n_\alpha - n_\beta} S_\alpha \tag{B.6}$$

From equation (B.5) we can write the entropy of the entire system as

$$S = \sum_{\beta \subseteq \Lambda} \tilde{S}_\beta \tag{B.7}$$

This is still an exact expression. The approximation that has to be introduced to obtain the CVM is based on the following observation: the cumulants $\tilde{S}_\alpha$ are expected to vanish quickly for clusters with linear size larger than the correlation length of the system. One is then led to define a set $M$ of clusters with the property that for any cluster $\alpha \in M$ all its subclusters $\beta \subset \alpha$ also belong to $M$. Clearly, such a set is uniquely determined by the set of 'maximal' clusters $\gamma_i$ which are not subclusters of any other element in $M$. The CVM approximation is then obtained by truncating (B.7) and keeping only terms belonging to $M$

$$S \simeq \sum_{\alpha \in M} \tilde{S}_\alpha \equiv \sum_{\alpha \in M} a_\alpha S_\alpha \tag{B.8}$$

The coefficient $a_\alpha$ in (B.8) obey

$$a_\alpha = \begin{cases} N_e(\alpha) - N_o(\alpha) & \text{if } n_\alpha \text{ even} \\ N_o(\alpha) - N_e(\alpha) & \text{if } n_\alpha \text{ odd} \end{cases} \tag{B.9}$$

where $N_e(\alpha)$ is the number of clusters in $M$ larger than or equal to $\alpha$ with even numbers of sites, and $N_o(\alpha)$ is similarly defined for the odd clusters. Alternatively the coefficient $a_\alpha$ can be determined from

$$\sum_{\{\beta : \alpha \subseteq \beta \in M\}} a_\beta = 1 \quad \forall \alpha \in M \tag{B.10}$$

The truncated functional for the free energy reads

$$F[\{\rho_\alpha, \alpha \in M\}] = \sum_{\alpha \in \Gamma} \mathrm{Tr}\ \rho_\alpha H_\alpha + (\kappa_B T) \sum_{\alpha \in M} a_\alpha \mathrm{Tr}\ (\rho_\alpha \ln \rho_\alpha) \tag{B.11}$$

where $H_\alpha$ is an $n_\alpha$-body interaction and $\Gamma$ is a collection of clusters such that the Hamiltonian $H$ can be written as

$$H = \sum_{\alpha \in \Gamma} H_\alpha \tag{B.12}$$

It usual to choose M such that all clusters of $\Gamma$, which define the range of interactions, are contained in $M$. However, in the usual mean field approximation one takes $M$ as the collection of all single sites regardless of $\Gamma$.

In actual applications, simple symmetry considerations often reduce the sum in (B.11) to a very small number of terms. The clusters in $M$ can generally be grouped into equivalence classes (i.e. all the bond in a certain direction, all the sites of a given sublattice, and so on) and the reduced free energy density functional reads

$$f[\{\rho_\alpha, \alpha \in M\}] = (\kappa_B T)^{-1} \sum_{\alpha \in M} \nu_\alpha \mathrm{Tr}\,(\rho_\alpha \mathcal{H}_\alpha) + \sum_{\alpha \in M} \nu_\alpha a_\alpha \mathrm{Tr}\,(\rho_\alpha \ln \rho_\alpha) \tag{B.13}$$

where now the index $\alpha$ refers to equivalence classes and $\nu_\alpha$ is the multiplicity (number of clusters per site) of each class in the thermodynamic limit.

The free energy functional $f$ has to be minimized with respect to the density matrices $\rho_\alpha$, subject to the constraints

$$\begin{aligned} &\mathrm{Tr}\ \rho_\alpha = 1, && \forall \alpha \in M \\ &\rho_\alpha = \mathrm{Tr}_{\beta/\alpha} \rho_\beta, && \forall \beta \in M \end{aligned} \tag{B.14}$$

A system on nonlinear algebraic equations is obtained, which can be solved numerically by Kikuchi's natural iteration algorithm [65, 66] or by other numerical methods.

# Bibliography


[1] P.J. Flory, *Principle of Polymers Chemistry*, Cornell University Press, Ithaca (1953).

[2] P.G. de Gennes, *Scaling Concepts in Polymer Physics*, (Cornell University Press, Ithaca 1988).

[3] J. des Cloizeaux and G. Jannink, *Polymers in solution: their modelling and structure* (Clarendon Press, Oxford, 1990).

[4] M. Plischke and B. Bergersen, *Equilibrium Statistical Mechanics* (World Scientific, Singapore,1994).

[5] C. Vanderzande, *Lattice models of polymers* (Cambridge University Press, Cambridge, 1998).

[6] C. Branden and J. Tooze, *Introduction to Protein Structure* (Garland Publishing, New York, 1991).

[7] H.S. Chan and K.A. Dill, Phys. Today **46**, 2, 24 (1993).

[8] K.A. Dill, S. Bromberg, K. Yue, K.M. Fiebig, D.P. Yee, P.D. Thomas, and H.S. Chan, Protein Sci. **4**, 561 (1995).

[9] S. Lise, J. Phys. **A31**, 6183 (1998).

[10] C. Micheletti, J.R. Banavar, A. Maritan and F. Seno, Phys. Rev. Lett. **80**, 5683 (1998).

[11] N. Madras and G. Slade, *The Self-Avoiding Walk*, (Birkhauser, Boston, 1993).

[12] A.R. Conway, and A.J. Guttmann, Phys. Rev. Lett. **77**, 5284 (1996).

[13] I.G. Enting, and A.J. Guttmann, J. Phys. A **22**, 1371 (1989).

[14] A.J. Guttmann, J. Phys. A **22**, 2807 (1989).

[15] P. Grassberger and R. Hegger, J. Phys. I (France) **5**, 597 (1995).

[16] M.C. Tesi, E.J. Janse van Rensburg, E. Orlandini, and S.G. Whittington, J. Stat. Phys. **82**, 155 (1996).

[17] P.G. de Gennes, J. Phys. Lett. (Paris) **36**, L55 (1975).

[18] B. Duplantier and H. Saleur, Phys. Rev. Lett. **59**, 539 (1987).

[19] B. Nienhuis, Phys. Rev. Lett. **49**, 1062 (1982).

[20] B. Li, N. Madras, and A.D. Sokal, J. Stat. Phys. **80**, 661 (1995).

[21] J.C. Le Guillou, and J. Zinn-Justin, J. Physique Lett. **46**, L137 (1985).

[22] B. Derrida and D. Stauffer, J. Physique (Paris), **46**, 1623 (1985).

[23] G. Parisi, and N. Sourlas, Phys. Rev. Lett. **46**, 871 (1981).

[24] K.F. Lau and K.A. Dill, Macromolecules **22**, 3986 (1989).

[25] H.S. Chan and K.A. Dill, Proteins: Struct. Funct. Genet. **34**, 335 (1996).

[26] R. Dekeyser, E. Orlandini, A.L. Stella and M.C. Tesi, Phys. Rev. **E52**, 5214 (1995).

[27] A.J. Guttmann, in *Phase transition and critical phenomena*, vol. 13, edited by C. Domb and J. Lebowitz, Academic Press (1989).

[28] V. Privman, J. Phys. **A19**, 3287 (1986).

[29] See discussion in F. Seno an C. Vanderzande, J. Phys. **A27**, 5813 (1994).

[30] J.F. Douglas and T. Ishinabe, Phys. Rev. **E51**, 1791 (1995).

[31] H. Orland, C. Itzykson, and C. de Dominicis, J. Phys. Lett. (Paris) **46**, 353 (1985).

[32] D.S. Gaunt and H. Ruskin, J. Phys. **A11**, 1369 (1978).

[33] K. Binder, *Monte Carlo and molecular dynamics simulations in polymer science*, Oxford University Press (1995).

[34] M. Lal, Mol. Phys. **17**, 57 (1969).

[35] N. Madras and A.D. Sokal, J. Stat. Phys. **56**, 109 (1988).

[36] F. Igloi, J. Phys. **A19**, 3077 (1986).

[37] B. Eynard, E. Guitter, and C. Kristjansen, *Hamiltonian Cycles on a Random Three-coordinate Lattice*, preprint cond-mat/9801281.

[38] J. Kondev and J.L. Jacobsen, *Conformational Entropy of Compact Polymers*, preprint cond-mat/9804048.

[39] S. Higuchi, *Hamiltonian cycles on random lattices of arbitrary genus*, preprint cond-mat/9806349.

[40] P.J. Flory, Proc. Roy. Soc. A **234**, 60, (1956).

[41] P.J. Flory, Proc. Natl. Acad. Sci. **79**, 4510 (1982).

[42] J. Bascle, T. Garel, and H. Orland, J. Phys. A **25**, L1323 (1992).

[43] B. Duplantier and F. David, J. Stat. Phys. **51**, 327 (1988).

[44] J.F. Nagle, P.D. Gujrati, and M. Goldstein, J. Chem. Phys. **88**, 4599 (1984).

[45] J. Bascle, T. Garel, and H. Orland, J. Phys. (France) I **3**, 259 (1993).

[46] J. Bascle, T. Garel, and H. Orland, J. Phys. (France) II **3**, 245 (1993).

[47] T. Garel, H. Orland, and D.Thirumalai, in *New developments in theoretical studies of proteins*, edited by R. Elber (World Scientific).

[48] P.G. de Gennes, Phys. Lett. **A38**, 339 (1972).

[49] T. Plefka, J. Phys. A **15**, 1971 (1982).

[50] A. Georges and J.S. Yedidia, J. Phys. A **24**, 2173 (1991).

[51] A.M. Nemirovsky, and M.D. Coutinho-Filho, J. Stat. Phys. **53**, 1139 (1988).

[52] M.T. Batchelor, H.W.J. Blote, B. Nienhuis, and C.M. Yung, J. Phys. **A29**, L399 (1996).

[53] M.T. Batchelor, J. Suzuki, and C.M Yung, Phys. Rev. Lett. **73**, 2646 (1994).

[54] E. Frey, K. Kroy, J. Wilhelm, and E. Sackmann, in *Dynamical networks in physics and biology*, edited by G. Forgacs and D. Beysens (EDP Sciences Springer Verlag, 1998).

[55] A.Y. Grosberg and D.V. Kuznetsov, Macromolecules **25**, 1970 (1992).

[56] J. Ubbink and T. Odijk, Biophys. J. **68**, 54 (1995).

[57] M. Muthukumar, J. Chem. Phys. **81**, 6272 (1984).

[58] U. Bastolla, and P. Grassberger, J. Stat. Phys. **89**, 1061 (1997).

[59] J.P.K. Doye, R.P. Sear, and D. Frenkel, J. Chem. Phys. **108**, 2134 (1998).

[60] S. Doniach, T. Garel, and H. Orland, J. Chem. Phys. **105**, 1601 (1996).

[61] S. Lise, A. Maritan and A. Pelizzola, preprint (1998).

[62] A. Kolinsky, J. Skolnick, and R. Yaris, J. Chem. Phys. **85**, 3585, (1986).

[63] A. Kolinsky, J. Skolnick, and R. Yaris, Proc. Natl. Acad. Sci. **83**, 7267 (1986).

[64] R. Kikuchi, Phys. Rev. **81**, 988 (1951).

[65] R. Kikuchi, J. Chem. Phys. **60**, 1071 (1974).

[66] R. Kikuchi, J. Chem. Phys. **65**, 4545 (1976).

[67] G. An, J. Stat. Phys. **52**, 727, (1988).

[68] See e.g. contributions in Progr. Theor. Phys. Suppl., **115** (1994).

[69] M.L. Huggins, Ann. N.Y. Acad. Sci. **43**, 1 (1942).

[70] J.H. Gibbs and E.A. Di Marzio, J. Chem. Phys. **28**, 373 (1958).

[71] A. Pelizzola, Phys. Rev. E **49**, R2503 (1994).

[72] A. Pelizzola, Physica A **211**, 107 (1994).

[73] P.D. Gujrati, J. Phys. A **13**, L437 (1980); J. Stat. Phys. **28**, 441 (1982).

[74] P.D. Gujrati, and M. Goldstein, J. Chem. Phys **74**, 2596 (1981).

[75] H. Saleur, j. Phys. A **19**, 2409 (1986).

[76] E. Orlandini, F. Seno, M.C. Tesi and A.L. Stella, Phys. Rev. Lett. **68**, 488 (1992).

[77] E. Orlandini and T. Garel, *Collapse transition of a periodic hydrophilic hydrophobic chain* preprint cond-mat/9807080.

# Acknowledgments

I would like to thank Amos Maritan for proposing me the arguments of this thesis and for helping and supervising me during the work.
I am grateful to the condensed matter group (and to SISSA in general) for the chance given. While in SISSA, moreover, I could appreciate the efficiency and the kindness of the secretaries.
During the Ph.D., I have had the pleasure to collaborate with Michael Swift, Attilio Stella, Henrik Jensen, Flavio Seno, Cristian Micheletti, Alessandro Pelizzola, Giuseppe Gonnella and Jayanth Banavar (whose name is always the last one). I have also enjoyed discussions with Antonio Trovato, Cecilia Clementi, Paolo De Los Rios, Jort van Mourik, Claudio Tebaldi and Matteo Marsili. I have greatly benefited from all of them.
I am particularly grateful to all my friends (some of them have been already 'cited' above) and to my family for their support.
Finally, I would like to remember Lando.